CLM-P611

CLM-P611

UKAEA

Preprint

ALLOWED AND FORBIDDEN n = 2 - 2 TRANSITIONS OF THE ELEMENTS Ti, Cr, Fe, Co AND Ni IN TOKAMAK DISCHARGES

K. D. LAWSON
N. J. PEACOCK
M. F. STAMP

CULHAM LABORATORY
Abingdon Oxfordshire

1981

CLM-P611

ALLOWED AND FORBIDDEN n = 2-2 TRANSITIONS OF THE ELEMENTS Ti, Cr, Fe, Co AND Ni IN TOKAMAK DISCHARGES

by

K.D.LAWSON*, N.J.PEACOCK and M.F.STAMP+

Culham Laboratory, Abingdon, Oxon., OX14 3DB, U.K.
(Euratom/UKAEA Fusion Association)

ABSTRACT

Wavelengths and transition probabilities are presented for the allowed and forbidden n = 2 - 2 transitions belonging to the fluorine I to lithium I isoelectronic sequences which are expected to be observed in tokamak discharges. The listing is compiled for the elements Ti, Cr, Fe, Co and Ni, these metals being likely contaminants. The emphasis is placed on an accurate compilation of wavelengths from laboratory and solar flare observations. Where these are inadequate, predictions are given. In the case of the nitrogen-, carbon- and boron-like intercombination lines, these predictions represent a significant improvement on previous data. Theoretical line intensities calculated for conditions typical of a tokamak plasma are given for each transition.

Identifications in Ti of the five strongest forbidden transitions lying in the visible and near-UV spectral regions have been made in spectra from the DITE tokamak. Such spectral features are useful diagnostic indicators of metallic ion impurity concentrations and mass motions.

Submitted to J.Phys. B: Atom.Molec.Phys.

* On attachment from Royal Holloway College, University of London.
+ On attachment from the University of Oxford.

March, 1980.

1. INTRODUCTION

Current interest in the allowed and forbidden n = 2 - 2 transitions of the metallic impurity elements in tokamak discharges results from their use for certain diagnostic purposes. For example, the intensities of these transitions allow measurements of the concentrations of impurity ions which originate in the high temperature interior of the discharge. Of particular interest are the forbidden transitions within the ground configurations. Whereas the allowed n = 2 - 2 transitions fall in the XUV spectral region, these forbidden transitions occur throughout the UV and visible regions. In addition to the other diagnostic applications, high resolution line profile measurements, allowing a study of Doppler effects, are possible with the longer wavelength forbidden lines.

It is, therefore, appropriate to list wavelengths of all the n = 2 - 2 transitions expected to be seen in tokamaks in order to facilitate their identification. Such a listing is presented for the elements titanium, chromium, iron, cobalt and nickel,these being the most likely metallic contaminants in hydrogen and helium plasmas. Titanium impurities result from its frequent use for gettering hydrogen, carbon and oxygen and from its use as current - aperture limiters in various machines. The other elements are components of the alloys from which the vacuum vessels are made.

The compilation of wavelengths uses available laboratory and solar flare observations and is given for the n = 2 - 2 transitions in the FI to LiI isoelectronic sequences. Where these data are incomplete, reliable predictions are given. Recent identifications in spectra of laser produced plasmas (Lawson and Peacock 1980a), in addition to providing many new boron- and beryllium- like observations, allow significant improvements to be made in the predictions of the wavelengths of the various nitrogen-, carbon- and boron- like intercombination lines. As will be discussed in section 3.5, the ambiguity regarding the separation of the doublet and quartet levels in the BI isoelectronic sequence which resulted from tentative identifications by Lawson and Peacock (1980a) has now been resolved.

In addition to the wavelengths listed, transition probabilities and theoretical line intensities calculated for conditions typical of a tokamak plasma are given for each transition. The transition probabilities

have been collected from a number of sources, that considered to be the most reliable, in each instance, being used. In cases where there is no published data available, the results of new calculations are presented. Although less accurate than the transition probabilities, the calculated intensities should be an aid to the identification of these transitions.

By using the listing of wavelengths and intensities, identifications have been made in spectra from the Divertor Injection Tokamak Experiment (DITE) and observations of all the forbidden transitions in titanium expected in the visible and near-UV spectral regions are reported. These identifications are supported by the good agreement between the predicted and measured wavelengths and intensities and by the observed dependence of their line intensities on the plasma temperature.

2. EXPERIMENTAL TECHNIQUES

Spectra of the DITE plasma were recorded on two instruments, one being a Rank Hilger, medium quartz prism spectrograph and the other a Rank Hilger, normal incidence, 1 meter grating spectrometer. The former was used to observe the spectra throughout the visible and in the near-UV spectral region down to a wavelength of about 2000Å. This range overlaps that of the grating spectrometer which was used for wavelengths below 2500Å. Additional optics were employed to focus the centre of the discharge onto the slit of the quartz prism spectrograph, the slit being adjusted to a width of 25μm, and Ilford HP3 and Q2 plates were used to record the spectra. The normal incidence instrument was set up with a grating ruled with 1200 lines mm^{-1} and a slit width of 50μm. Photographic records of the spectra were made on SC5 film, this enabling accurate wavelengths to be measured. A photoelectric attachment to the normal incidence instrument gave the time behaviour of particular spectral lines.

The wavelength measurements were made from a number of spectra and records were the result of multiple exposures of, typically, ten discharges. These spectra were taken under a variety of plasma conditions and, consequently, the dependence of the line intensities on plasma temperature could be noted. The identified titanium lines were found to be intense in deuterium and helium discharges characterised by high ohmic heating currents and neutral hydrogen beam heating. In these experiments, the heating current was varied up to 220 kA and, when used, the total power of the injected neutral beams was typically 0.9MW.

These conditions correspond to peak electron temperatures of about 0.8 to 1.5keV. The electron density was typically $1.5 \times 10^{13} cm^{-3}$. Below a threshold of about 100kA heating current, the lines disappeared from the spectra.

Mass motion effects resulting in Doppler shifts are expected to be most severe during neutral beam injection due to momentum transfer from the beam atoms. However, comparisons of spectra taken both with and without neutral beam injection showed that for the highly ionised titanium lines any such shifts were smaller than the quoted wavelength accuracies. These accuracies depend chiefly on the nearness of suitable calibration lines, carbon, oxygen and weakly-ionised titanium lines being used for this purpose.

3. COMPILATION OF WAVELENGTHS AND THEORETICAL DATA

The listings of wavelengths, transition probabilities and estimates of line intensities is presented in tables 1 - 7. This compilation is comprehensive tin that it includes all the allowed and forbidden n = 2 - 2 transitions of the metallic impurity elements likely to be found in tokamak discharges which are expected to have an observable intensity. The choice of which transitions to include was determined from their theoretical line intensities, all possible electric and magnetic dipole and electric quadrupole transitions being considered.

Where possible, the wavelengths given are those of laboratory and solar flare observations and the tables are completed with reliable predictions. In a few cases, the reliability of the observed wavelengths is in question and predictions are preferred. Accurate semi-empirical calculations are now available for the FI, OI, BeI and LiI isoelectronic sequences (Edlén,1979a,b, 1980). These calculations involve a smoothing of the observed values along an isoelectronic sequence of transitions and, since this reduces random experimental errors, the results are to be preferred to the original observations. In the other sequences, much use is made of the laboratory wavelengths listed by Fawcett (1975) and Lawson and Peacock (1980a) and of the solar flare observations recorded in the NRL Apollo Telescope Mount experiments on Skylab.

These data were also used in making the wavelength predictions. Those for the forbidden transitions within the ground configurations were found by graphically smoothing the wavenumbers derived from the term schemes of Fawcett (1975) and Lawson and Peacock (1980a). The smoothing was achieved by extrapolating the differences of consecutive wavenumbers along an isoelectronic

sequence, the observations of the forbidden transitions, where available, being included unaltered in the extrapolations. Adjustments, which, on the whole were found to be small, were made to the resulting smoothed values so that they were consistent with the Rydberg-Ritz combination principle. Modified term schemes were then completed using the observed laboratory wavelengths and predictions of transitions between configurations were calculated from these term schemes. In this way, reliable wavelengths were obtained for all the transitions of interest. Detailed references to the various sources of data used are given in the tables.

As an aid to making identifications, estimates of the wavelength accuracies are presented for both observations and predictions. For the majority of observations, these values are as given in the original source. However, where this data is unavailable or is questionable, alternative estimates are suggested.

As with the listed wavelengths, the transition probabilities are selected from a number of sources, those considered to be the most reliable being adopted. In many instances where there are differences between the sources used, there is no decisive reason for preferring any one set of results. Generally, in these cases, the most complete set is used, the size of the discrepancies being noted in the text. Of the sources, the listings of Bhatia et al (1980) and Feldman et al (1979,1980), in many cases, show good agreement with other published values and, since they are the most comprehensive, much data is taken from these references. Where no data has been published, as, for example, is the case for nearly all transitions in cobalt, Hartree-X self-consistent field calculations (Cowan and Griffin 1976) have been used to provide new data. Since comparisons of the results of these calculations with published energy levels and transition probabilities indicate some significant discrepancies, the output of the computer code has been adjusted to fit those transition probabilities which are regarded as being more reliable. This adjustment involved multiplying the Hartree-X output by a factor required to give agreement between other transitions in the same isoelectronic sequence. In general, the transition probabilities of the strongest allowed transitions are thought to be the most reliable, whereas there is greatest uncertainty in the values for weak forbidden transitions. However, as will be discussed in the following sections, the mixing of energy levels can lead to very significant uncertainties and reference should be made to the appropriate section for the details of the effect of this mixing on the transition probabilities.

Because of the very significant departures from a statistical population of the energy levels in tokamak plasmas, the transition probabilities give little indication of the strength of the line emission. Consequently, it was thought valuable to present theoretical line intensities of each transition. It should be emphasised, however, that since the intensities depend on model calculations of level populations, their values are expected to be less accurate than the transition probabilities.

The line intensities were calculated from the formulae $I = \frac{1}{4\pi} N_j A_{ij}$ photons sec^{-1} sr^{-1} per ion number, where A_{ij} is the transition probability of the spontaneous radiative decay $j \rightarrow i$ and N_j is the fraction of the total ion number found in level j. N_j is dependent on the electron density and, ignoring excitation by proton collisions, less strongly on temperature. Values for N_j, calculated for an electron density of $4 \times 10^{13} cm^{-3}$, have been taken from the model calculations of Bhatia et al.(1980) and Feldman et al (1979,1980). The electron temperature is that for which the abundances of the particular ion species is a maximum under ionisation equilibrium. The calculations include electron collisional excitation and de-excitation and spontaneous radiative decay between levels within the $2s^n 2p^k$ configurations. An initial comparison of calculations which also include excitation and de-excitation by proton collisions suggests a somewhat poorer agreement with experiment than if these processes are excluded (Suckewer and Hinnov 1979); consequently, the populations obtained without proton interactions have been used. Whatever further comparisons reveal with regard to proton collisions in ohmically heated discharges, it is likely that they will be much more important during neutral beam injection. It is also worth noting that the effect of including proton excitations is, in any case, comparatively small in the calculations of Bhatia et al.(1980) and Feldman et al (1979,1980), this contrasting with the independent calculations of Suckewer and Hinnov (1979). This difference arises chiefly from the larger electron collisional excitation rates used in the former calculations, there being no great difference in the proton excitation rates between these separate calculations.

3.1. FI Isoelectronic Sequence

The allowed transitions in the FI isoelectronic sequence are well known in all the elements considered. The semi-empirical calculations of Edlén (1980), the results of which are listed in table 1, give particularly accurate wavelengths; these can be used as provisional wavelength standards in the XUV spectral region.

The forbidden $2s^2 2p^5 ({}^2P_{3/2} - {}^2P_{\frac{1}{2}})$ transition in iron has been observed in a solar flare and in the Princeton Large Torus (PLT) tokamak (Suckewer and Hinnov 1979) and an identification is given for this transition in titanium.

3.2. OI Isoelectronic Sequence

As in the FI isoelectronic sequence, the allowed transitions are well known from observations in laser produced plasmas and the results of the semi-empirical calculations of Edlén (1980) are given in table 2. Some of the forbidden transitions within the $2s^2 2p^4$ ground configurations in iron and nickel have been observed in solar flares and the $2s^2 2p^4 ({}^3P_2 - {}^3P_1)$ transition in titanium is identified in DITE spectra.

There is good agreement between the transition probabilities of Bhatia et al (1980), Feldman et al (1980) and those of Kastner et al (1977) and the oscillator strengths listed by Fawcett (1978), all of these calculations being, typically, within 10% of each other. Since the first two named are the most comprehensive, preference has been given to these sources in compiling the lists of transition probabilities.

3.3. NI Isoelectronic Sequence

The majority of $2s^2 2p^3 - 2s2p^4$ transitions of interest have been observed in laser produced plasmas and it is these wavelengths which are given in table 3. This table, also, details the magnetic dipole transitions in iron and nickel that have been seen in solar flares and in the PLT tokamak.

The transition probabilities of Feldman et al(1979) and Kastner et al(1977) and the oscillator strengths of Fawcett (1978) agree well, in most cases, with the results of Bhatia and Mason (1980), Bhatia et al (1980) and Feldman et al (1980), the differences, typically, being smaller than 10%. Transition probabilities from the latter references are used in table 3.

In the cases where there are discrepancies, it is found that one of the energy levels involved in the transition interacts strongly with one or more other levels of the same parity and total angular momentum. This is seen as a significant mixing of the LS terms which compose the levels and it can have a strong influence on the strength of the transitions to and from these levels, particularly if the levels cross. As the interaction between the levels

probabilities become significant. If transitions from two interacting levels to one other level are considered, then in one case, the relative signs of the contributions are such that they add, thereby increasing the line strength and, in the other, the contributions cancel. Consequently, the transition probabilities can vary quite markedly with Z and, near a crossing of levels, it is possible for the probability of one transition to show a pronounced maximum, the other vanishing. This behaviour is illustrated for the crossing of the $2s2p^{22}S_{\frac{1}{2}}$ and $2s^{2}3s^{2}S_{\frac{1}{2}}$ levels in the BI isoelectronic sequence by Dankwort and Trefftz (1977); the probabilities of the transitions from these levels to the $2s^{2}2p^{2}P_{\frac{1}{2}}$ ground state exhibit the features described.

The interaction of energy levels can lead to significant errors in the calculation of transition probabilities for two different reasons. Firstly, cancellation of contributions to the line strength that are of a similar magnitude will, necessarily, lead to the percentage error being increased; this most affects those transitions whose probabilities become very small or vanish. A further uncertainty arises because different calculations place the point at which the energy levels cross or at which the interaction is maximum at different values of Z. This, in turn, affects the position of the maximum or minimum of the transition probabilities. If the probability varies rapidly with Z, then even small displacements of the turning points can result in significantly different predictions for a particular element.

In the NI isoelectronic sequence, there are three pairs of interacting levels in the elements being considered, these being the $2s^{2}2p^{3}\ ^{2}D_{3/2}$ and $^{2}P_{3/2}$ levels in the ground configurations and the $2s2p^{42}D_{3/2}$ and $^{2}P_{3/2}$ and $2s2p^{4}\ ^{2}P_{\frac{1}{2}}$ and $^{2}S_{\frac{1}{2}}$ levels in the singly excited configurations. However, none of these interactions is resolved by a simple crossing of the levels as Z increases; instead, the mixing becomes complicated by significant contributions from the respective quartet terms.

Although the calculated probabilities for all transitions to and from these pairs of levels are likely to be less reliable than for other transitions, a comparison of the results available for the NI sequence suggests that only four of the transitions included in the listing will be seriously affected. These are the forbidden $2s^{2}2p^{3}(^{4}S_{3/2}-^{2}D_{3/2})$ transition and those within the $2s^{2}2p^{3}-2s2p^{4}$ transition array with terms $^{2}P_{\frac{1}{2}}-^{2}P_{\frac{1}{2}}$, $^{2}P_{3/2}-^{2}S_{\frac{1}{2}}$ and $^{2}D_{5/2}-^{2}D_{3/2}$.

For the first three, the results of Fawcett(1978) are typically 15% lower than the results of the other references listed above. There is strong cancellation of the contributions to the line strengths of the last of these transitions and the discrepancies are found to be larger. In chromium and iron Fawcett's results are, respectively, 30% and 75% lower than those of Feldman et al (1980) and Bhatia and Mason (1980). The sharp fall in the line strengths means that this transition will only have an observable intensity in titanium and chromium. The probabilities given by Bhatia and Mason (1980), Bhatia et al (1980) and Feldman et al (1980) are used for these transitions. It should be noted that, although there is good agreement with the results of Feldman et al (1979) and, where a comparison can be made, with the more elaborate calculations of Kastner et al (1977), all these calculations use the same computer code and, consequently, the discrepancies with the semi-empirical results of Fawcett may give a more realistic indication of the reliability of the listed transition probabilities.

3.4. CI Isoelectronic Sequence

Observed wavelengths are given for most of the $2s^2 2p^2 - 2s2p^3$ transitions included in the listing. The position of the $^5S_2$ level in low Z elements is only known in neon (Ridgeley and Burton 1972) and, consequently, the wavelength predictions for the $^3P_{1,2} - ^5S_2$ transitions in titanium are particularly dependent on the identifications of these transitions in calcium (Lawson and Peacock 1980b). All other wavelength predictions are thought to be reliable. Magnetic dipole transitions in titanium and iron have been observed,respectively, in the PLT tokamak (Bhatia et al 1980) and solar flares. Since no wavelength accuracy is given for the PLT observation, the wavelength of the titanium transition as measured in DITE spectra is preferred. A further identification in DITE spectra is that of the $2s^2 2p^2 (^3P_0 - ^3P_1)$ transition in titanium.

Most of the ab initio data available for the n = 2 - 2 transitions are results of non-relativistic multiconfigurational Hartree-Fock calculations to which relativistic corrections have been added. It is, therefore, of interest to be able to compare these results with other ab initio calculations which are based on a different approach. This is the perturbation theory used by Safronova (1975b), which involves expansions in powers of 1/Z. The results for the CI sequence are presented by Bogdanovich et al(1978) and comparisons of the wavelengths and energy levels for FeXXI shows that the agreement with experiment is generally better than is found for any of the Hartree-Fock

calculations. It should be noted that this is not clear in the comparison made by Bogdanovich et al., since less experimental data was then available. Although the variational procedures used in the Hartree-Fock methods result in more accurate wave functions, these methods only accurately give the first term in the $^1/Z$ expansion. The use of the perturbation theory, which allows further terms of this expansion to be satisfactorily calculated, would appear in the case of FeXXI to more than compensate for the use of the less exact wave functions; in fact, hydrogen-like wave functions were used in these perturbation theory calculations. It is interesting to note that the effect of configurational interaction between the $2s^2 2p^2$ and $2p^4$ configurations is already accounted for in the first order perturbation theory. Other comparisons with the results of the perturbation theory are made for transitions in the BeI isoelectronic sequence and are discussed in section 3.6. The perturbation theory results for the OI sequence (Safronova 1975a) cannot be compared directly with the listed probabilities, since for that particular sequence Safronova's results are in pure LS coupling, whereas it is necessary to use intermediate coupling for an adequate description of states in these elements.

The Hartree-Fock results available for the CI sequence are listed by Bhatia et al.(1980), Feldman et al.(1979,1980) and Mason et al.(1979) and papers dealing only with the forbidden transitions include those of Kastner et al.(1977) and Nussbaumer and Rusca (1979). The transition probabilities given by these authors were compared with the perturbation theory results (Bogdanovich et al. 1978) and with the semi-empirical oscillator strengths of Fawcett (1978), whose calculations are, again, based on a Hartree-Fock approach. The agreement, in many cases, was found to be within 10% and this gives confidence in the values of the transition probabilities listed in this paper.

In all but one case, the exceptions appear to be due to the mixing of energy levels. The effect of this on the line strengths is discussed in section 3.3. In these elements, the largest interaction occurs between the $2s^2 2p^2\ ^3P_2$ and $^1D_2$ levels, which, in fact, cross at higher Z. A result of this interaction is that contributions to the probability of the $2s^2 2p^2\ ^3P_2$-$2s2p^3\ ^3D_2$ transition cancel, this probability vanishing near manganese. The $2s^2\ 2p^2\ ^3P_2$-$2s2p^3\ ^3D_1$ transition also shows subtraction, whereas the $2s^2 2p^2\ ^1D_2$-$2s2p^3\ ^3P_1$, $^3P_2$ transitions are strengthened, the latter, in particular, having a sharp maximum. There is also mixing between other energy levels, notably the $2s2p^3\ ^3S_1$ and $^1P_1$ and the $2s2p^3\ ^3D_2$ and $^3P_2$ levels. In these cases,

components of other terms with equal J become significant as Z increases. Although the accuracy of the probabilities of all transitions to and from these levels may be less certain than for transitions between levels free from mixing, the comparison between the various results suggest that only a few transitions are affected. For those within the $2s^2 2p^2 - 2s2p^3$ transition array with terms $^3P_o - ^3S_1$, $^3P_2 - ^1D_2$, $^3P_1 - ^3P_2$ and $^3P_2 - ^3P_1$, there are discrepancies, typically, of 15%. For the $2s^2 2p^2\ ^3P_2 - 2s2p^3\ ^3D_1$, $^3D_2$ and $2s^2\ p^2\ ^1D_2 - 2s2p^3\ ^3P_2$ transitions, the differences are larger, being up to 40% of the values listed in table 4.

A further discrepancy, which does not appear to be due to level mixing, is found for the $2s^2 2p^2\ ^3P_1 - 2s2p^3\ ^5S_2$ transition. Fawcett's (1978) calculations give results up to 30% larger than those of the other calculations, for all of which there is good agreement. The reason for the discrepancy is not clear. It may reflect the difficulty in dealing with intercombination lines or it may be a consequence of the lack of experimental data for positioning the $2s2p^3\ ^5S_2$ level, this only being known in neon when the calculations were made.

For the transitions for which discrepancies have been noted, there are no decisive reasons for preferring any one set of data. Consequently, the transition probabilities of Bhatia et al (1980), Feldman et al(1980) and Mason et al (1979) have been used for all the electric dipole transitions, these results forming the most comprehensive listing available. For the forbidden transitions within the $2s^2 2p^2$ ground configurations, the transition probabilities of Nussbaumer and Rusca (1979) are given, since they are considered to be the most accurate available. There is, in any case, good agreement between all the results for the forbidden transitions.

3.5. BI Isoelectronic Sequence

Nearly all the allowed transitions listed for the BI isoelectronic sequence have been observed in laser produced plasmas and their wavelengths are given in table 5. The forbidden $2s^2 2p(^2P_{\frac{1}{2}} - ^2P_{3/2})$ transition in iron has been observed both in a solar flare and the PLT tokamak. The wavelength of the solar flare observation, 845.4±0.2Å(Noyes 1972), which has been misquoted in some of the literature, is in good agreement with the laboratory wavelength of 845.55±0.1Å. The latter is used because of its smaller uncertainty. This transition in titanium is newly observed in DITE spectra and the predictions

of Edlén (1977) for the other elements in this sequence of forbidden transitions have been adjusted to fit the tokamak observation of iron.

The position of the ^4P levels in this sequence have been determined using the same procedure as described for the levels within the ground configurations, the wavenumbers of all the $2s^2 2p - 2s2p^2$ intercombination lines being graphically smoothed and then adjusted to fit the Rydberg-Ritz combination principle. This has, in fact, allowed the ambiguity regarding the separation of the doublet-quartet levels to be resolved. Lawson and Peacock (1980a) tentatively identified a sequence of spectral lines observed in laser produced plasmas with the $2s2p^2\ ^4P_{5/2} - 2p^3\ ^2D_{5/2}$ transition, noting that the only wavelength predictions close to the observations were for the $2s2p^2\ ^4P_{5/2} - 2p^3\ ^2D_{5/2,3/2}$ transitions. Given these alternatives, only the identification with the $^4P_{5/2} - ^2D_{5/2}$ transition is found to be acceptable. If the other identification is assumed correct and term schemes derived, then the extrapolation of the wavenumbers of the $2s^2 2p^2 P_{3/2} - 2s2p^2\ ^4P_{\frac{1}{2}}$ transition is found to bave a sharp maximum. Further evidence comes from calculations of the intensities of the lines within the $2s2p^2\ ^4P - 2p^3\ ^2D$ multiplet. At the high electron densities of a laser produced plasma, typically 10^{20-21} cm^{-3}, the intensity of the $^4P_{5/2} - ^2D_{5/2}$ transition is expected to be about 50 times greater than that of the $^4P_{5/2} - ^2D_{3/2}$ transition. Consequently, the doublet-quartet level separation can be fixed, the error, x, in table 13 of Lawson and Peacock (1980a) being zero, and unambiguous wavelength predictions of the intercombination lines derived. These predictions are preferred to the tentative identifications of some of these lines in solar flares (Sandlin et al 1976), the latter not having entirely satisfactory relative intensities or level splittings.

For completeness, the possibility of the sequence of lines in the spectra of the laser produced plasmas being identified with the only other intense transition in the $2s2p^2\ ^4P - 2p^3\ ^2D$ multiplet was considered. This is the $^4P_{3/2} - ^2D_{3/2}$ transition, which is expected to have about half the intensity of the $^4P_{5/2} - ^2D_{5/2}$ transition. In addition to the wavelength predictions being less satisfactory, it would be expected that a sequence of lines corresponding to the more intense $^4P_{5/2} - ^2D_{5/2}$ transition would, also, be seen in the spectra. No such sequence is observed.

For the BI sequence, the listings of transition probabilities by Bhatia et al (1980) and Feldman et al. (1979, 1980) were compared with those by Mason and Storey (1980) and Dankwort and Trefftz (1978) and the oscillator strengths

of Fawcett (1978). For many of the transitions good agreement was found, the differences being, typically, less than 10%. As was found in the CI sequence, the most serious discrepancies are for transitions to or from energy levels which cross; in this sequence, the $2s2p^2\ ^2P_{\frac{1}{2}}$ and $^2S_{\frac{1}{2}}$ levels cross near vanadium and the $2s2p^2\ ^2P_{3/2}$ and $^2D_{3/2}$ are expected to cross at higher Z. It should be noted that despite the largest contribution to the $2s2p^2\ ^2P_{\frac{1}{2}}$ and $^2S_{\frac{1}{2}}$ levels being reversed in some of the elements considered, the labelling has not been changed. This means that there is continuity of the isoelectronic extrapolations and, in fact, it is consistent with that used in much of the literature.

On considering the effect of the level crossings on the transition probabilities, it is found that the $2s2p^2\ ^2P_{\frac{1}{2}}$ and $^2S_{\frac{1}{2}}$ levels behave differently in their transitions to the two ground states; the $2s^22p\ \ ^2P_{\frac{1}{2}}$-$2s2p^2\ ^2P_{\frac{1}{2}}$ and $2s^22p\ \ ^2P_{3/2}$-$2s2p^2\ ^2S_{\frac{1}{2}}$ transitions show subtraction, the probability of the latter vanishing near chromium, while the $2s^22p\ \ ^2P_{3/2}$-$2s2p^2\ ^2P_{\frac{1}{2}}$ and $2s^22p\ \ ^2P_{\frac{1}{2}}$-$2s2p^2\ ^2S_{\frac{1}{2}}$ transitions are increased in intensity. In the case of the $2s2p^2\ ^2P_{3/2}$ and $^2D_{3/2}$ levels, it is the $2s^22p\ \ ^2P_{3/2}$-$2s2p^2\ ^2D_{3/2}$ transition which vanishes and this occurs near cobalt. Since the various calculations differ about the precise positions of the vanishing points, there are considerable discrepancies for the $2s^22p\ \ ^2P_{3/2}$-$2s2p^2\ ^2S_{\frac{1}{2}}$,$^2D_{3/2}$ transitions. For example, for these transitions in iron, the results of Feldman et al(1979), whose calculations consider only the three configurations $2s^22p$,$2s2p^2$ and $2p^3$, are, respectively, more than on order of magnitude lower and double those of the most elaborate calculations of Mason and Storey (1980). In these cases, the probabilities of Dankwort and Trefftz (1978) are used in table 5, since they are in reasonable agreement with the data of Mason and Storey (1980) and, in most cases, with that of Fawcett (1978) and are considered more reliable than the probabilities of Bhatia et al.(1980) and Feldman et al(1979,1980). Excluding the latter references, typical discrepancies are of about 30% of the values given, although Fawcett's result for the $^2P_{3/2}$-$^2S_{\frac{1}{2}}$ transition in titanium exceeds that of Dankwort and Trefftz by 55%.

For all other transitions, the probabilities given by Bhatia et al(1980) and Feldman et al(1979,1980) are used, this including the other transition to show subtraction, the $2s^22p\ \ ^2P_{\frac{1}{2}}$-$2s2p^2\ ^2P_{\frac{1}{2}}$ transition, for which there is also significant discrepancies. In this case, these results are intermediate to the other data available and the differences are within 30% of the listed values. Discrepancies are also found between the probabilities available for the $2s^22p\ \ ^2P_{3/2}$-$2s2p^2\ ^4P$ transitions; those listed in table 5 are in good

agreement with the results of Dankwort and Trefftz (1978) but differ by upto 25% from some of the other data. This is probably due to the difficulties of treating intercombination lines, which are particularly sensitive to relativistic and mixing effects, there being some mixing of the $2s2p^2\ ^4P_{\frac{1}{2}}$ and $^4P_{5/2}$ levels with other levels of equal J.

3.6 BeI Isoelectronic Sequence

The BeI isoelectronic sequence is the only one in which transitions between singly and doubly excited configurations are expected to have observable intensities. The electron density in tokamaks is too small for a significant population to be excited to the levels within the doubly excited configurations in the other sequences. The wavelengths given for the electric dipole transitions listed in table 6 are those calculated by the semi-empirical procedure of Edlén (1980).

The ground configuration in this sequence consists of a single ^1S_o term and, consequently, the only magnetic dipole transitions likely to be observed will be in the singly excited 2s2p configuration. Mühlethaler and Nussbaumer(1976) find the probability of the $2s2p(^3P_1-^3P_2)$ transition to be three orders of magnitude greater than the alternative decay channel from the $2s2p\ ^3P_2$ level, this being the magnetic quadrupole transition to the $2s^2\ ^1S_o$ ground state. The $2s2p(^3P_1-^3P_2)$ transition in titanium is newly identified in DITE spectra.

As in the CI isoelectronic sequence, a comparison can be made between the transition probabilities calculated by the 1/Z perturbation theory of Victorov and Safronova (1977) and the results of the multiconfigurational Hartree-Fock calculations, which for the BeI sequence are given by Bhatia et al (1980), Feldman et al (1980) and Mühlethaler and Nussbaumer (1976). As before, the semi-empirical calculations of Fawcett (1978) are included in the comparison and the agreement is, typically, better than 10%. The one exception is for the $2s^2\ ^1S_o$-$2s2p\ ^3P_1$ transition for which Fawcett (1978) and Victorov and Safronova (1977), respectively, give values which exceed the other results by, typically, 20% and 40%. The results of Glass (1979), whose calculations are based on Hartree-Fock methods, are intermediate to those of Feldman et al(1980) and Mühlethaler and Nussbaumer (1976) and those of Victorov and Safronova (1977). As for the intercombination lines in the BI sequence, these differences are thought to be due to the sensitivity of this line to level mixing and relativistic effects. The comprehensive results of Bhatia et al (1980) and Feldman et al (1980) are given for all transitions in this sequence, although

it should be noted that these results may underestimate the probabilities of the $2s^2\ ^1S_0$-$2s2p\ ^3P_1$ transition.

3.7. LiI Isoelectronic Sequence

The lithium-like doublets of several fourth period elements have been observed in laboratory and solar flare plasmas and semi-empirical calculations by Edlén (1979a,b)are available for these transitions. The results of these calculations are given in table 7.

In this sequence, collision strengths and level populations are only available for titanium and, consequently, intensity estimates are given only for this element. However, it is expected that the intensities for the other elements considered will not be substantially different from the values given for titanium.

4. SPECTRAL CLASSIFICATIONS AND DISCUSSION

The use of titanium for gettering in the DITE tokamak and as a fabricant for the current-aperture limiter results in a relatively high concentration of this metallic impurity and its allowed spectral lines are clearly observed in the XUV spectral region. A search was, therefore, made of visible and near-UV DITE spectra for titanium magnetic dipole transitions. In fact, all of the lines expected to have an observable intensity were identified. The identifications of these forbidden lines, are listed in table 8.

Confidence in these identifications stems not only from the good agreement between the observed and predicted wavelengths and intensities, but also from the temperature dependence and temporal variation of the line intensities. As already discussed in section 2, the line intensities were found to depend on the plasma temperature, as indicated by the ohmic heating current and the power of the injected neutral beam. The temporal variation of the intensities of the $2s^2 2p^5(^2P_{3/2}$-$^2P_{\frac{1}{2}})$ and $2s^2 2p(^2P_{\frac{1}{2}}$-$^2P_{3/2})$ transitions at the beginning of the discharge are shown in figure 1, together with those of a CIII and an OVII transition. The ohmic heating current is indicative of the temperature rise, the peak electron temperature having a value of 710eV,80 ms after the current initiation. The appearance and burn through time of each ion depends on its ionisation potentials and the temporal variation of the titanium lines is consistent with their identification as Ti XIV and Ti XVIII. In addition, these temporal intensities have been compared with the results of an ionisation model calculation, in which a uniform volume of titanium plasma is subjected to a temperature rise which follows the ohmic heating current. The resulting relative ion populations as a function of time are found to be in

good agreement, having appropriately corrected for ion diffusion, with the observed line emissions from the DITE tokamak.

Some of these titanium lines have also been studied in the Poloidal Divertor Experiment (PDX) at Princeton (Suckewer et al., 1980). † Although there is overall agreement between the results, two small discrepancies are noted. The fluorine-like $2s^2 2p^5 (^2P_{3/2} - ^2P_{\frac{1}{2}})$ transition, reported as having a wavelength of 2115.3±0.5Å by Suckewer et al., is observed at a somewhat longer wavelength of 2117.07±0.08Å in the DITE spectra. The latter wavelength is in good agreement with the semi-empirical prediction of Edlén (1977). Also, the wavelength of the carbon-like $2s^2 2p^2 (^3P_o - ^3P_1)$ transition is measured as 3370.6±0.1Å, in contrast to the PDX observation of 3371.5±0.5Å. A line at 3371.5Å in the DITE spectra is identified with a TiI transition.

Figure 2 shows a spectrum obtained from the DITE tokamak of the UV spectral region around a wavelength of 2000Å. It can be seen that the fluorine- and boron- like magnetic dipole transitions in titanium are intense, being clearly seen against the background, and are well separated from other spectral features. Given that high resolution spectroscopic techniques (Breton et al.1980) can be used at these wavelengths and that this spectral region is experimentally less demanding than the XUV region, where the allowed transitions are observed, it can be appreciated that these lines are ideal for diagnostic purposes. In some cases, the interest lies in the fact that the high ionisation stages only originate in and are, therefore, characteric of the high temperature interior of the discharge; for example, forbidden line profiles have been used to measure mass motions and the ion temperatures in the PLT tokamak (Suckewer et al.1979, Suckewer and Hinnov 1978, Eubank et al.1978). In other cases, a knowledge of the atomic physics is necessary, as when, for example, ion concentrations are derived from absolute line intensities or from the temporal variation in intensity due to charge exchange during the injection of neutral beams (Afrosimov et al.1978).

For ease of reference to the tables 1-7, Grotian diagrams are presented for titanium in figure 3.

5.CONCLUSION

In this paper, we present wavelengths, transition probabilities and theoretical

† A more recent reassessment of these wavelengths (Suckewer 1980) indicates much closer agreement with the data in Table I.

intensities for all the allowed and forbidden n = 2 - 2 transitions in the FI to LiI isoelectronic sequences which are expected to have an observable intensity in tokamak discharges. This listing is made for titanium, chromium, iron, cobalt and nickel, which are the most likely metallic impurity elements. Where possible the wavelengths are those of laboratory or solar flare observations, the listing being completed with reliable predictions. The transition probabilities are the results of theoretical calculations and are drawn from various sources. Those expected to be the most reliable are used and, in cases where no clear choice can be made, the size of any discrepancy is indicated. For some transitions, no data is available and the results of new calculations are given.

The usefulness of the data presented is demonstrated by the ready identification of all the forbidden titanium lines expected to be seen in the visible and near-UV spectral regions, in spectra observed in the DITE tokamak. Although all the n = 2 - 2 transitions can be used for some diagnostic measurements, the long wavelength forbidden lines are of particular interest, since they fall in spectral regions where high resolution spectroscopy can be used. A prerequisite of some of the diagnostic techniques is a knowledge of the radiative transition probabilities, for which this listing will also be appropriate.

ACKNOWLEDGEMENTS

The authors wish to acknowledge our collaboration with S.J.Fielding and other members of the DITE group in this study. We would also like to thank H.Gordon both for useful discussions and for assistance in running the Hartree-X computer code and J.Payne for running the ionisation model calculation. In addition, we have received copies of papers prior to publication from B.Edlén, U.Feldman and H.E.Mason which have proved to be particularly valuable to the preparation of this paper.

REFERENCES.

V.V.AFROSIMOV, Yu.S.GORDEEV, A.N.ZINOV'EV and A.A.KOROTKOV, 1978, JETP Lett., 28, pp 500-2.

A.K.BHATIA and H.E.MASON, 1980, Astron. Astrophys., 83, pp 380-2.

A.K.BHATIA, U.FELDMAN and G.A.DOSCHEK, 1980, J.Appl.Phys., 51, pp 1464-80.

P.O.BOGDANOVICH, G.V.MERKELIS, Z.B.RUDZIKAS, S.D.ŠADŽIUVIENE and U.I. SAFRONOVA, 1978, Physica Scripta, 17, pp.549-55.

C.BRETON, C.De MICHELIS, M.FINKENTHAL and M.MATTIOLI, 1980, J.Phys.E,13, pp.216-21.

R.D.COWAN and D.C.GRIFFIN, 1976, J.Opt.Soc.Am.,66, pp.1010-4.

W.DANKWORT and E.TREFFTZ, 1977, J.Phys.B, 10, pp.2541-52.

W.DANKWORT and E.TREFFTZ, 1978, Astron.Astrophys., 65, pp.93-8.

K.P.DERE, 1978, Astrophys.J., 221, pp.1062-7.

B.EDLÉN, 1972, Solar Phys. 24, pp.356-67.

B.EDLÉN, 1977, Opt.Pura Apl.,10, pp.123-9.

B.EDLÉN, 1979a, Physica Scripta, 19, pp.255-66.

B.EDLÉN, 1979b, Physica Scripta, 20, pp 129-37.

B.EDLÉN, 1980, to be published in Physica Scripta.

H.EUBANK et al., 1978, Proc.7th Int.Conf.on Plasma Physics and Controlled Nuclear Fusion, 1, IAEA (1979), pp.167-98.

B.C.FAWCETT, 1975, Atomic Data and Nuclear Data Tables, 16, pp.135-64.

B.C.FAWCETT, 1978, Atomic Data and Nuclear Data Tables, 22, pp.473-89.

B.C.FAWCETT, M.GALANTI and N.J.PEACOCK, 1974, J.Phys.B, 7, pp.1149-53.

U.FELDMAN, G.A.DOSCHEK, R.D.COWAN and L.COHEN, 1975, Astrophys.J., 196, pp.613-6.

U.FELDMAN, G.A.DOSCHEK, CHUNG-CHIEH CHENG and A.K.BHATIA, 1979. Private communication.

U.FELDMAN, G.A.DOSCHEK, CHUNG-CHIEH CHENG and A.K.BHATIA, 1980. J.Appl. Phys., 51, pp.190-201.

R.GLASS, 1979, J.Phys.B, 12, pp.697-703.

S.O.KASTNER, A.K.BHATIA and L.COHEN, 1977, Physica Scripta, 15, pp.259-67.

K.D.LAWSON and N.J.PEACOCK, 1980a, J.Phys.B, 13, pp 3313-34.

K.D.LAWSON and N.J.PEACOCK, 1980b, to be submitted to Astron.Astrophys.

H.E.MASON and P.J.STOREY, 1980, to be published in Astron.Astrophys.

H.E.MASON, G.A.DOSCHEK, U.FELDMAN and A.K.BHATIA, 1979, Astron. Astrophys., 73, pp.74-81.

H.P.MÜHLETHALER, and H.NUSSBAUMER, 1976, Astron.Astrophys., 48, pp.109-14.

R.W.NOYES, 1972, Proc. Symposium on High Energy Phenomena on the Sun, ed.R Ramaty and R.G.Stone, NASA SP-342(1973), pp.231-41.

H.NUSSBAUMER and C.RUSCA, 1979, Astron.Astrophys., 72, pp.129-33.

A.RIDGELEY and W.M.BURTON, 1972, Solar Phys., 27, pp.280-5.

U.I.SAFRONOVA, 1975a, J.Quant.Spectrosc.Radiat.Transfer, 15, pp.223-9. (In Russian).

U.I. SAFRONOVA, 1975b, J.Quant.Spectrosc.Radiat.Transfer, 15, pp.231-42. (In Russian).

G.D.SANDLIN, G.E.BRUECKNER, V.E.SCHERRER and R.TOUSEY, 1976, Astrophys. J., 205, pp.L47-50.

G.D.SANDLIN, G.E.BRUECKNER and R.TOUSEY, 1977, Astrophys.J., 214, pp.898-904.

S.SUCKEWER, 1980, Private communication.

S.SUCKEWER and E.HINNOV, 1978, Phys. Rev.Lett., 41, pp.756-9.

S.SUCKEWER and E.HINNOV, 1979, Phys.Rev.A, 20, pp.578-85.

S.SUCKEWER, H.P.EUBANK, R.J.GOLDSTON, E.HINNOV and N.R.SAUTHOFF, 1979. Phys.Rev.Lett., 43, pp.207-10.

S.SUCKEWER, R.FONCK and E.HINNOV, 1980, Phys.Rev.A, 21, pp.924-7.

D.S.VICTOROV and U.I.SAFRONOVA, 1977, J.Quant.Spectrosc.Radiat.Transfer, 17, pp605-11.

K.G.WIDING, 1978, Astrophys.J., 222, pp.735-9.

TABLE I. Wavelengths, Transition Probabilities and Theoretical Intensities of Transitions Isoelectronic with Fluorine I

Transition $2s^2 2p^5 - 2s2p^6$	Ti XIV λ	Ti XIV A	Ti XIV I	Cr XVI λ	Cr XVI A	Cr XVI I	Fe XVIII λ	Fe XVIII A	Fe XVIII I	Co XIX λ	Co XIX A	Co XIX I	Ni XX λ	Ni XX A	Ni XX I
$^2P_{3/2} - {}^2S_{\frac{1}{2}}$	121.98 A	6.5+10 a	8.9+2 d	106.63 A	6.9+10 b	6.2+2 e	93.92 A	8.5+10 b	4.2+2 e	88.34 A	9.4+10 c	3.3+2 f	83.18 A	1.04+11 b	2.5+2 e
$^2P_{\frac{1}{2}} - {}^2S_{\frac{1}{2}}$	129.44 A	2.7+10 a	3.7+2 d	115.35 A	2.8+10 b	2.5+2 e	103.94 A	3.2+10 b	1.6+2 e	99.00 A	3.4+10 c	1.19+2 f	94.50 A	3.6+10 b	8.6+1 e
$2s^2 2p^5$															
$(^2P_{3/2} - {}^2P_{\frac{1}{2}})$	2117.07±0.08 B 2117.74±0.08	1.9+3 a	4.1+1 d	1410.8±0.4 D	6.1+3 b	1.33+2 e	974.86±0.05 C	1.8+4 b	3.3+2 e	820.0±0.2 D	3.1+4 c	4.8 +2 f	694.54±0.15 D	5.0+4 b	6.8+2 e

Wavelengths given in Å.
Estimated wavelength accuracy is better than + 0.01Å unless otherwise stated.
Wavelengths above 2000Å are in air (Vacuum wavelength given in brackets).
Transition probabilities given in sec^{-1}.
Theoretical intensities have units of photons $sec^{-1} sr^{-1}$ per ion number.
Theoretical intensities are calculated for an electron density of $4 \times 10^{13} cm^{-3}$ and for the temperature of maximum ion abundance under ionisation equilibrium.

A - Calculated values of Edlén (1980).
B - New laboratory observation.
C - Solar flare observation of Sandlin et al.(1977)
D - Predictions of Edlén (1977).
a - Transition probabilities listed by Bhatia et al (1980).
b - Transition probabilities listed by Feldman et al(1980)
c - Transition probabilities found using data from Feldman et al (1980) in conjunction with own calculations.
d - Theoretical intensities obtained from data of Bhatia et al(1980).
e - Theoretical Intensities obtained from data of Feldman et al (1980).
f - Theoretical intensities found by graphical interpolation.

TABLE 2. Wavelengths, Transition Probabilities and Theoretical Intensities of Transitions Isoelectronic with Oxygen I

Transition $2s^2 2p^4 - 2s2p^5$	Ti XV λ	Ti XV A	Ti XV I	Cr XVII λ	Cr XVII A	Cr XVII I	Fe XIX λ	Fe XIX A	Fe XIX I	Co XX λ	Co XX A	Co XX I	Ni XXI λ	Ni XXI A	Ni XXI I
$^3P_2 - {}^1P_1$	102.24 A	4.8+9 a	1.9+1 e	89.60 A	7.7+9 c	1.17+1 f	78.89 A	1.12+10 c	7.1+0 f	74.10 A	1.30+10 c	5.9+0 g	69.63 A	1.48+10 c	4.9+0 f
$^1D_2 - {}^1P_1$	115.03 A	1.20+11 a	4.7+2 e	101.93 A	1.37+11 b	2.1+2 f	91.02 A	1.6+11 b	9.8+1 f	86.19 A	1.7+11 d	7.5+1 g	81.70 A	1.7+11 b	5.7+1 f
$^1S_0 - {}^1P_1$	131.14 A	9.0+9 a	3.5+1 e	117.21 A	1.02+10 b	1.5+1 f	106.11 A	1.13+10 b	7.2+0 f	101.39 A	1.20+10 d	5.4+0 g	97.14 A	1.26+10 b	4.1+0 f
$^3P_2 - {}^3P_1$	134.63 A	1.9+10 a	2.9+2 e	116.59 A	2.4+10 b	2.1+2 f	101.55 A	3.2+10 b	1.7+2 f	94.93 A	3.6+10 d	1.5+2 g	88.82 A	4.2+10 b	1.37+2 f
$^3P_1 - {}^3P_0$	138.36 A	4.2+10 a	1.9+2 e	120.89 A	5.0+10 b	1.08+2 f	106.32 A	6.1+10 b	4.6+1 f	99.88 A	6.7+10 d	2.7+1 g	93.92 A	7.4+10 b	1.36+1 f
$^3P_2 - {}^3P_2$	140.39 A	2.9+10 a	8.4+2 e	122.96 A	3.4+10 b	5.8+2 f	108.35 A	3.9+10 b	4.4+2 f	101.88 A	4.3+10 d	4.0+2 g	95.86 A	4.6+10 b	3.6+2 f
$^3P_1 - {}^3P_1$	142.13 A	9.5+9 a	1.43+2 e	125.42 A	1.11+10 b	9.4+1 f	111.69 A	1.29+10 b	6.8+1 f	105.71 A	1.37+10 d	5.8+1 g	100.24 A	1.46+10 b	4.8+1 f
$^3P_0 - {}^3P_1$	142.74 A	1.21+10 a	1.8+2 e	125.06 A	1.40+10 b	1.18+2 f	109.95 A	1.6+10 b	8.7+1 f	103.16 A	1.8+10 d	7.5+1 g	96.80 A	1.9+10 b	6.3+1 f
$^3P_1 - {}^3P_2$	148.59 A	8.4+9 a	2.5+2 e	132.82 A	9.6+9 b	1.6+2 f	119.98 A	1.07+10 b	1.21+2 f	114.41 A	1.13+10 d	1.06+2 g	109.31 A	1.19+10 b	9.3+1 f
$^1D_2 - {}^3P_2$	165.70 A	8.2+8 a	2.4+1 e	147.45 A	1.35+9 c	2.3+1 f	132.62 A	2.0+9 c	2.3+1 f	126.21 A	2.4+9 c	2.3+1 g	120.35 A	2.9+9 c	2.2+1 f
$^1S_0 - {}^3P_1$	189.64 A	2.7+8 a	4.0+0 e	168.14 A	4.8+8 c	4.0+0 f	151.60 A	7.3+8 c	3.9+0 f	144.88 A	8.5+8 c	3.6+0 g	139.07 A	9.4+8 c	3.1+0 f

TABLE 2. (Continued) Wavelengths, Transition Probabilities and Theoretical Intensities of Transitions Isoelectronic with Oxygen I

Transition $2s^2 2p^4$	Ti XV			Cr XVII			Fe XIX			Co XX			Ni XXI		
	λ	A	I	λ	A	I	λ	A	I	λ	A	I	λ	A	I
$(^3P_1 - {}^1S_o)$	567.35±0.10 F	2.2+4 a	3.4+1 e	493.59±0.09 F	5.6+4 b	2.6+1 f	424.25±0.06 E	1.32+5 b	1.7+1 f	391.04±0.08 F	2.0+5 d	1.21+1 g	358.99±0.07 F	2.9+5 b	7.2+0 f
$(^3P_2 - {}^1D_2)$	919.3±0.3 F	2.3+3 a	4.1+1 e	740.4±0.2 F	6.4+3 b	7.0+1 f	592.21±0.06 C	1.6+4 b	9.2+1 f	528.46±0.14 F	2.6+4 d	9.4+1 g	471.13±0.06 E	4.0+4 b	7.5+1 f
$(^3P_1 - {}^1D_2)$	1438.7±0.6 F	2.2+2 a	3.9+0 e	1339.1±0.7 F	4.1+2 b	4.5+0 f	1259.1±0.3 G	6.8+2 b	3.8+0 f	1223.8±0.7 F	8.4+2 d	3.0+0 g	1190.8±0.7 F	1.02+3 b	1.9+0 f
$(^3P_2 - {}^3P_1)$	2545.08±0.08 B (2545.84±0.08)	1.26+3 a	2.3+1 e	1656.2±1.1 F	4.4+3 b	7.4+1 f	1118.07±0.05 D	1.38+4 b	1.37+2 f	930.1±0.4 F	2.3+4 d	1.5+2 g	779.6±0.3 F	3.9+4 b	1.6+2 f

Wavelengths given in Å.
Estimated wavelength accuracy is ± 0.01Å unless otherwise stated.
Wavelengths above 2000Å are in air (Vacuum wavelength given in brackets).
Transition probabilities given in sec^{-1}.
Theoretical intensities have units of photons $sec^{-1} sr^{-1}$ per ion number.
Theoretical intensities are calculated for an electron density of $4 \times 10^{13} cm^{-3}$ and for the temperature of maximum ion abundance under ionisation equilibrium.

A-- Calculated values of Edlén (1980).
B - New laboratory observation.
C - Solar flare observation of Dere(1978), Sandlin et al(1976) and Widing (1978).
D - Solar flare observation of Sandlin et al(1977).
E - Solar flare observations of Sandlin et al(1976) and Widing(1978).
F - Predictions of Edlén (1980).
G - Prediction made using data from sources B and C.
a - Transition probabilities listed by Bhatia et al(1980).
b - Transition probabilities listed by Feldman et al(1980).
c - Transition probabilities found using data from Bhatia et al(1980) in conjunction with own calculations.
d - Transition probabilities found using data from Feldman et al(1980)in conjunction with own calculations.
e - Theoretical intensities obtained from data of Bhatia et al(1980).
f - Theoretical intensities obtained from data of Feldman et al(1980) together with transition probabilities as referenced.
g - Theoretical intensities found by graphical interpolation.

TABLE 3. Wavelengths, Transition Probabilities and Theoretical Intensities of Transitions Isoelectronic with Nitrogen I

Transition $2s^2 2p^3 - 2s2p^4$	Ti XVI λ	Ti XVI A	Ti XVI I	Cr XVIII λ	Cr XVIII A	Cr XVIII I	Fe XX λ	Fe XX A	Fe XX I	Co XXI λ	Co XXI A	Co XXI I	Ni XXII λ	Ni XXII A	Ni XXII I
$^4S_{3/2} - {}^2P_{3/2}$	102.38 K	1.12+9 b	6.8+0 f	90.63 C	2.3+9 d	7.5+0 h	80.50 C	4.3+9 a	7.7+0 g	75.87 C	5.5+9 d	7.2+0 j	71.50 C	6.9+9 d	6.0+0 h
$^2D_{3/2} - {}^2P_{1/2}$	110.57 A	3.5+10 b	4.2+1 f	95.77 C	3.2+10 c	2.5+1 h	83.25 C	3.0+10a	7.3+0 g	77.68 C	2.9+10e	3.0+0 j	72.52 C	2.8+10 c	1.5+0 h
$^2D_{3/2} - {}^2P_{3/2}$	116.21 A	1.5+10 b	9.3+1 f	102.32 C	1.6+10 c	5.3+1 h	90.60 C	1.6+10a	2.8+1 g	85.39 C	1.49+10e	2.0+1 j	80.54 C	1.36+10 c	1.18+1 h
$^2D_{3/2} - {}^2P_{3/2}$	118.23 A	7.7+10 b	4.7+2 f	104.98 C	9.0+10 c	2.9+2 h	93.79 C	1.04+11a	1.9+2 g	88.77 C	1.12+11e	1.47+2 j	84.07 C	1.21+11 c	1.05+2 h
$^2D_{3/2} - {}^2S_{1/2}$	121.39 B	2.4+10 b	7.4+1 f	106.83 C	3.4+10 c	5.3+1 h	94.65 C	4.5+10 a	3.4+1 g	89.25 C	5.1+10 e	2.6+1 j	84.23 C	5.7+10 c	2.0+1 h
$^2P_{1/2} - {}^2P_{1/2}$	121.54 A	6.0+9 b	7.1+0 f	105.92 C	5.3+9 c	4.1+0 h	92.63 C	4.6+9 a	1.14+0 g						
$^2P_{3/2} - {}^2P_{1/2}$	124.81 A	6.2+10 b	7.3+1 f	110.41 C	8.1+10 c	6.2+1 h	98.37 C	1.00+11a	2.4+1 g	93.00 C	1.10+11 e	1.15+1 j	88.00 C	1.21+11 c	6.4+0 h
$^2P_{1/2} - {}^2P_{3/2}$	128.39 A	5.7+9 b	3.4+1 f	114.00 C	7.2+9 c	2.3+1 h	101.83 C	9.3+9 a	1.7+1 g	96.35 C	1.06+10 e	1.39+1 j	91.20 C	1.21+10 c	1.05+1 h
$^2P_{3/2} - {}^2P_{3/2}$	132.04 A	4.3+9 b	2.6+1 f	119.21 C	9.4+9 c	3.0+1 h	108.82 C	9.9+9 a	1.8+1 g	104.28 C	1.03+10 e	1.35+1 j	100.11 C	1.07+10 c	9.3+0 h
$^4S_{3/2} - {}^2D_{3/2}$	122.95±0.05 K	1.5+8 b	1.7+0 f	108.36 C	5.5+8 d	3.6+0 h	95.93 C	1.7+9 a	5.3+0 g	90.32 C	2.6+9 d	5.8+0 j	85.03 C	4.0+9 d	6.5+0 h

TABLE 3(Continued)Wavelengths, Transition Probabilities and Theoretical Intensities of Transitions Isoelectronic with Nitrogen 1

Transition $2s^2 2p^3 - 2s2p^4$	Ti XVI λ	Ti XVI A	Ti XVI I	Cr XVIII λ	Cr XVIII A	Cr XVIII I	Fe XX λ	Fe XX A	Fe XX I	Co XXI λ	Co XXI A	Co XXI I	Ni XXII λ	Ni XXII A	Ni XXII I
$^2P_{\frac{1}{2}} - {}^2S_{\frac{1}{2}}$	134.74 A	2.7+10 b	8.2+1 f	119.62 C	3.2+10 c	5.0+1 h	106.98 C	3.8+10 a	2.9+1 g	101.29 C	4.1+10 e	2.1+1 j	95.96 C	4.5+10 c	1.6+1 h
$^2P_{3/2} - {}^2S_{\frac{1}{2}}$	138.77 A	8.6+9 b	2.6+1 f	125.38 C	5.5+9 c	8.5+0 h	114.71 C	3.1+9 a	2.3+0 g	110.09 C	2.2+9 e	1.12+0j			
$^2D_{3/2} - {}^2D_{3/2}$	143.45 A	2.8+10 b	3.1+2 f	125.51 C	3.5+10 c	2.3+2 h	110.64 C	4.3+10 a	1.36+2g	104.14 C	4.7+10 e	1.06+2j	98.15 C	5.2+10 c	8.4+1 h
$^2D_{5/2} - {}^2D_{5/2}$	145.65 A	2.4+10 b	4.7+2 f	128.10 C	2.8+10 c	2.6+2 h	113.35 C	3.3+10 a	1.5+2 g	106.76 C	3.6+10 e	1.06+2 j	100.61 C	3.9+10 c	6.7+1 h
$^2D_{5/2} - {}^2D_{3/2}$	146.54±0.07 K	6.2+8 b	6.9+0 f	129.54±0.05 J	3.0+8 c	2.0+0 h									
$^4S_{3/2} - {}^4P_{\frac{1}{2}}$	157.81 A	1.30+10 b	2.8+2 f	136.52 C	1.6+10 c	3.2+2 h	118.66 C	2.1+10 a	2.7+2 g	110.71 C	2.3+10 e	2.6+2 j	103.31 C	2.6+10 c	2.6+2 h
$^4S_{3/2} - {}^4P_{3/2}$	161.17 A	1.20+10 b	5.5+2 f	139.87 C	1.48+10 c	6.1+2 h	121.83 C	1.8+10a	5.3+2 g	113.70 C	2.1+10 e	5.0+2 j	106.04 C	2.3+10 c	4.9+2 h
$^4S_{3/2} - {}^4P_{5/2}$	169.74 A	1.02+10 b	8.5+2 f	149.80 C	1.17+10 c	9.2+2 h	132.85 C	1.33+10 a	7.5+2 g	125.15 C	1.41+10 e	7.3+2 j	117.91 C	1.49+10 c	7.2+2 h
$^2P_{\frac{1}{2}} - {}^2D_{3/2}$	162.48 A	2.7+9 b	3.0+1 f	143.55 C	2.9+9 c	1.9+1 h	127.86 C	3.1+9 a	9.8+0 g	120.91 C	3.1+9 e	7.0+0 j	114.44 C	3.1+9 c	5.1+0 h
$^2P_{3/2} - {}^2D_{5/2}$	167.19 A	4.9+9 b	9.6+1 f	149.94 C	5.6+9 c	5.1+1 h	136.05 C	6.3+9 a	2.9+1 g	130.02 C	6.7+9 e	2.0+1 J	124.47 C	7.0+9 c	1.19+1 h
$^2P_{3/2} - {}^2D_{3/2}$	168.36±0.09 K	4.3+8 b	4.9+0 f	151.92±0.07 J	6.4+8 c	4.2+0 h	139.07±0.06 J	7.4+8 a	2.4+0 g	133.66±0.05 J	7.5+8 e	1.7+0 j	128.82±0.05 J	7.0+8 c	1.13+0 h

TABLE 3.(Continued)Wavelengths,Transition probabilities and Theoretical Intensities of Transitions Isoelectronic with Nitrogen 1

Transition $2s^2 2p^3 - 2s2p^4$	Ti XVI λ	Ti XVI A	Ti XVI I	Cr XVIII λ	Cr XVIII A	Cr XVIII I	Fe XX λ	Fe XX A	Fe XX I	Co XXI λ	Co XXI A	Co XXI I	Ni XXII λ	Ni XXII A	Ni XXII I
$^2D_{3/2} - {}^4P_{1/2}$				164.90±0.08 J	1.15+8 d	2.2+0 h	142.02±0.06 J	2.9+8 a	3.9+0 g	132.22±0.05 J	4.3+8 d	4.8+0 j	123.32±0.05 J	6.2+8 d	6.0+0 h
$^2D_{3/2} - {}^4P_{5/2}$	211.45±0.14 K	8.6+7 b	7.2+0 f	184.67±0.10 J	2.4+8 d	1.9+1 h	162.83±0.08 J	5.9+8 a	3.3+1 g	153.35±0.07 J	8.6+8 d	4.4+1 j	144.72±0.06 J	1.24+9 d	6.0+1 h
$^2D_{5/2} - {}^4P_{5/2}$	218.24±0.14 K	7.1+7 b	5.9+0 f	193.54±0.11 J	1.40+8 d	1.09+1h	173.43±0.09 J	2.5+8 a	1.43+1 g	164.60±0.08 J	3.3+8 d	1.7+1 j	156.51±0.07 J	4.3+8 d	2.1+1 h
$^2P_{1/2} - {}^4P_{1/2}$				197.52±0.11 J	1.02+8 d	2.0+0 h	171.69±0.09 J	2.4+8 a	3.2+0 g	160.48±0.08 J	3.5+8 d	4.0+0 j	150.20±0.07 J	5.2+8 d	5.1+0 h
$^2P_{3/2} - {}^4P_{3/2}$	249.3±0.2 K	6.1+7 b	2.8+0 f	222.04±0.15 J	1.09+8 d	4.5+0 h	201.01±0.12 J	1.8+8 a	5.1+0 g	192.14±0.11 J	2.1+8 d	5.2+0 j	184.04±0.10 J	2.6+8 d	5.5+0 h
$2s^2 2p^3$															
$(^4S_{3/2} - {}^2P_{3/2})$	455.8±0.4 J	7.0+3 b	4.3+1 f	377.9±0.3 J	1.48+4 c	4.7+1 h	309.25±0.03 E	2.7+4 a	3.0+1 g	278.5±0.2 J	3.5+4 e	2.0+1 j	250.2±0.2 J	4.4+4 c	1.01+1 h
$(^4S_{3/2} - {}^2P_{1/2})$	505.4±0.5 J	4.5+3 b	1.9+1 f	442.1±0.4 J	1.19+4 c	3.2+1 h	384.2±0.4 J	3.0+4 a	4.2+1 g	357.0±0.3 J	4.6+4 e	4.1+1 j	330.9±0.3 J	7.1+4 c	3.5+1 h
$(^4S_{3/2} - {}^2D_{5/2})$	763.8±0.9 J	7.4+1 b	1.7+0 f	662.8±0.7 J	3.2+2 c	5.2+0 h	567.81±0.06 G	1.23+3a	1.7+1 g	522.2±0.4 J	2.3+3 e	2.4+1 j	478.08±0.06 F	4.2+3 c	3.3+1 h
$(^4S_{3/2} - {}^2D_{3/2})$	860.5±1.5 J	1.9+3 b	2.6+1 f	793.3±1.3 J	5.9+3 c	6.4+1 h	721.48±0.11 L	1.6+4 a	1.25+2g	680.6±1.2 J	2.5+4 e	1.46+2j	636.6±1.0 J	3.9+4 c	1.23+2 h

TABLE 3.(Continued)Wavelengths,Transition probabilities and Theoretical Intensities of Transitions Isoelectronic with Nitrogen 1

Transition $2s^2 2p^3$	Ti XVI λ	A	I	Cr XVIII λ	A	I	Fe XX λ	A	I	Co XXI λ	A	I	Ni XXII λ	A	I
$(^2D_{3/2}-{}^2P_{3/2})$	969.4±0.9 J	4.5+3 b	2.8+1 f	721.9±0.8 J	1.40+4 c	4.4+1 h	541.35±0.06 H	4.1+4 a	4.4+1 g	471.4±0.4 J	6.7+4 e	3.6+1 j	412.2±0.4 J	1.09+5 c	2.5+1 h
$(^2D_{5/2}-{}^2P_{3/2})$	1130.5±1.3 J	1.7+3 b	1.02+1f	879.4±1.2 J	4.4+3 c	1.40+1 h	679.29±0.12 L	1.11+4a	1.21+1 g	596.9±0.7 J	1.7+4 e	9.5+0 j	524.9±0.7 J	2.7+4 c	6.1+0 h
$(^2D_{3/2}-{}^2P_{1/2})$	1225.1±1.5 J	1.35+3b	5.6+0 f	998.6±1.5 J	2.9+3 c	8.0+0 h	821.8±1.4 J	5.5+3 a	7.8+0 g	750.7±1.1 J	7.1+3 e	6.3+0 j	689.2±1.2 J	8.7+3 c	4.3+0 h
$(^2D_{3/2}-{}^2D_{5/2})$				4030±20 J (4030±20)	1.40+2 c	2.3+0 h	2665.1±0.3 D (2665.9±0.3)	4.5+2 a	6.0+0 g	2242±10 J (2243±10)	7.2+2 e	7.5+0 j	1920±9 J	1.10+3 c	8.6+0 h

Wavelengths given in Å.
Estimated wavelength accuracy is + 0.03Å unless otherwise stated.
Wavelengths above 2000Å are in air (Vacuum wavelengths given in brackets).
Transition probabilities given in sec^{-1}.
Theoretical intensities have units of photons $sec^{-1}sr^{-1}$per ion number.
Theoretical intensities are calculated for an electron density of $4 \times 10^{13} cm^{-3}$ and for the temperatures of maximum ion abundance under ionisation equilibrium.

A - Laboratory observations listed by Fawcett (1975).
B - Laboratory observation of Feldman et al(1975).
C - Laboratory observations listed by Lawson and Peacock (1980a).
D - Laboratory observation of Suckewer and Hinnov (1978).
E - Solar flare observation from Dere(1978), Lawson and Peacock (1980b) and Sandlin et al(1976).
F - Solar flare observation from Lawson and Peacock (1980b) and Widing (1978).
G - Solar flare observation from Widing (1978) and sources as for E.
H - Solar flare observation of Widing (1978).
J - Predictions made using data from Edlén (1972) and Lawson and Peacock(1980a) and appropriate solar flare and tokamak observations.
K - Predictions made using data from sources A and J.
L - Predictions calculated from wavelengths of observations D, F and H.

a - Transition probabilities given by Bhatia and Mason (1980).
b - Transition probabilities listed by Bhatia et al (1980).
c - Transition probabilities listed by Feldman et al (1980).
d - Transition probabilities found using data from Bhatia and Mason (1980) and Bhatia et al (1980) in conjunction with own calculations.
e - Transition probabilities found using data from Bhatia and Mason (1980) and Feldman et al(1980) in conjunction with own calculations.
f - Theoretical intensities obtained from data of Bhatia et al (1980).
g - Theoretical intensities obtained from data of Feldman et al (1979) together with transition probabilities as referenced.
h - Theoretical intensities obtained from data of Feldman et al(1980) together with transition probabilities as referenced.
j - Theoretical intensities found by graphical interpolation.

TABLE 4. Wavelengths, Transition Probabilities and Theoretical Intensities of Transitions Isoelectronic with Carbon I

Transition $2s^2 2p^2 - 2s2p^3$	Ti XVII λ	Ti XVII A	Ti XVII I	Cr XIX λ	Cr XIX A	Cr XIX I	Fe XXI λ	Fe XXI A	Fe XXI I	Co XXII λ	Co XXII A	Co XXII I	Ni XXIII λ	Ni XXIII A	Ni XXIII I
$^3P_1 - ^1P_1$	109.40 J	2.1+9 a	8.5+0 f	95.87 C	3.5+9 e	4.8+0 h	84.26 C	5.2+9 c	2.3+0 g	78.98 C	6.1+9 e	1.48+0 j			
$^3P_o - ^3S_1$	119.29 A	8.3+9 a	8.6+1 f	104.19 C	9.3+9 b	6.5+1 h	91.28 C	1.02+10 c	4.4+1 g	85.44 C	1.06+10 e	3.6+1 j	79.98 C	1.10+10 b	2.9+1 h
$^3P_1 - ^3S_1$	123.66 A	2.4+10 a	2.4+2 f	109.64 C	2.6+10 b	1.8+2 h	97.88 C	2.7+10 c	1.18+2 g	92.61 C	2.8+10 e	9.5+1 j	87.66 C	2.9+10 b	7.6+1 h
$^3P_2 - ^3S_1$	127.78 A	4.8+10 a	5.0+2 f	113.97 C	5.6+10 b	3.9+2 h	102.22 C	6.6+10 c	2.8+2 g	96.88 C	7.1+10 e	2.4+2 j	91.83 C	7.7+10 b	2.0+2 h
$^1D_2 - ^1P_1$	124.57 A	5.3+10 a	2.1+2 f	110.37 C	6.2+10 b	8.4+1 h	98.36 C	7.2+10 c	3.3+1 g	93.02 C	7.8+10 e	1.9+1 j	88.11 C	8.4+10 b	9.8+0 h
$^3P_2 - ^1D_2$	126.63±0.05 J	2.9+9 a	3.2+1 f	111.87 C	5.3+9 e	2.5+1 h	99.07 C	8.4+9 c	1.5+1 g	93.13 C	1.00+10 e	1.38+1 j	87.50 C	1.15+10 e	1.28+1h
$^1D_2 - ^1D_2$	141.96 A	4.0+10 a	4.6+2 f	126.33 C	4.5+10 b	2.1+2 h	113.30 C	5.0+10 c	9.0+1 g	107.49 C	5.2+10 e	7.1+1 j	102.08 C	5.5+10 b	6.1+1 h
$^1S_o - ^1P_1$	142.57 A	1.42+10a	5.7+1 f	126.30 C	1.6+10 b	2.2+1 h	112.47 C	1.9+10 c	8.6+0 g	106.23 C	2.0+10 e	5.0+0 j	100.42 C	2.2+10 b	2.6+0 h
$^3P_o - ^3P_1$	146.85±0.07 J	3.9+9 a	9.7+1 f	125.94 C	4.2+9 b	6.2+1 h	108.12 C	4.5+9 c	4.2+1 g	100.14 C	4.6+9 e	3.2+1 j	92.75 C	4.7+9 b	2.2+1 h
$^3P_1 - ^3P_2$	152.17±0.07 J	1.11+9 a	4.5+1 f	132.11 C	7.8+8 b	1.9+1 h	115.15 C	4.4+8 c	5.4+0 g	107.57 C	3.8+8 e	2.8+0 j	100.50 C	1.6+8 b	1.00+0 h

TABLE 4.(Continued) Wavelengths,Transition Probabilities and Theoretical Intensities of Transitions Isoelectronic with Carbon 1

Transition $2s^2 2p^2 - 2s2p^3$	Ti XVII λ	Ti XVII A	Ti XVII I	Cr XIX λ	Cr XIX A	Cr XIX I	Fe XXI λ	Fe XXI A	Fe XXI I	Co XXII λ	Co XXII A	Co XXII I	Ni XXIII λ	Ni XXIII A	Ni XXIII I
$^3P_1 - ^3P_1$	153.54 A	8.4+9 a	2.1+2 f	133.99 C	1.19+10 b	1.8+2 h	117.51 C	1.7+10 c	1.6+2 g	110.14 C	2.0+10 e	1.39+2 j	103.23 C	2.4+10 b	1.11+2 h
$^3P_1 - ^3P_0$	154.09 B	1.6+10 a	1.39+2 f	134.89 C	2.0+10 b	9.5+1 h	118.69 C	2.4+10 c	6.5+1 g	111.47 C	2.6+10 e	4.3+1 j	104.70 C	2.9+10 b	1.9+1 h
$^3P_2 - ^3P_2$	158.46 A	1.37+10 a	5.5+2 f	138.45 C	1.7+10 b	4.2+2 h	121.21 C	2.2+10 c	2.6+2 g	113.37 C	2.5+10 e	1.8+2 j	106.02 C	2.9+10 b	1.7+2 h
$^3P_2 - ^3P_1$	159.94 A	3.7+9 a	9.2+1 f	140.51 C	3.5+9 b	5.2+1 h	123.82 C	3.2+9 c	3.0+1 g	116.23 C	3.0+9 e	2.1+1 j	109.06 C	2.8+9 b	1.31+1 h
$^3P_0 - ^3D_1$	172.22±0.09 J	6.4+9 a	2.3+2 f	148.65 C	8.9+9 b	2.6+2 h	128.73 C	1.23+10c	3.7+2 g	119.93 C	1.45+10e	4.3+2 j	111.85 C	1.7+10 b	4.8+2 h
$^3P_1 - ^3D_1$	181.49±0.10 J	1.29+9 a	4.6+1 f	159.99 C	1.11+9 b	3.2+1 h	142.26 C	8.3+8 c	2.5+1 g	134.56 C	6.8+8 e	2.0+1 j	127.47 C	5.1+8 b	1.45+1 h
$^3P_1 - ^3D_2$	182.08 A	6.7+9 a	5.1+2 f	160.30 C	8.3+9 b	3.5+2 h	142.16 C	1.01+10c	2.7+2 g	134.13 C	1.11+10e	1.9+2 j	126.54 C	1.21+10b	9.5+1 h
$^3P_2 - ^3D_3$	188.31 A	5.4+9 a	5.5+2 f	165.46 C	6.1+9 b	4.0+2 h	145.65 C	6.8+9 c	2.1+2 g	136.75 C	7.2+9 e	1.7+2 j	128.30 C	7.7+9 b	1.44+2 h
$^3P_2 - ^3D_1$							151.62±0.07 G	6.9+7 c	2.1+0 g	143.77±0.06 G	1.17+8 e	3.5+0 j	136.47±0.06 G	1.9+8 b	5.5+0 h
$^3P_2 - ^3D_2$	191.16±0.11 J	9.8+7 a	7.5+0 f												
$^1D_2 - ^3P_2$	183.23±0.10 J	9.4+7 a	3.8+0 f	161.31±0.08 G	1.7+8 e	4.2+0 h	143.22±0.06 G	2.0+8 c	2.4+0 g	135.39±0.06 G	1.7+8 e	1.28+0 j			
$^1D_2 - ^3P_1$	185.21±0.10 J	1.9+8 a	4.6+0 f	164.11±0.08 G	2.7+8 e	4.0+0 h	146.88±0.07 G	2.9+8 c	2.7+0 g	139.49±0.06 G	2.6+8 e	1.8+0 j			
$^1D_2 - ^3D_3$	224.35±0.15 J	3.1+8 a	3.2+1 f	199.19±0.12 G	6.0+8 e	4.0+1 h	178.64±0.10 G	1.02+9 c	3.1+1 g	170.12±0.09 G	1.27+9 e	2.9+1 j	162.32±0.08G	1.5+9 e	2.9+1 h
$^1D_2 - ^3D_1$	227.5±0.2 J	6.2+7 a	2.2+0 f	204.91±0.13 G	1.23+8 e	3.6+0 h	187.71±0.11 G	2.0+8 c	6.2+0 g	181.12±0.10 G	2.4+8 e	7.3+0 j	175.61±0.09G	2.8+8 e	8.0+0 h

TABLE 4.(Continued) Wavelengths, Transition Probabilities and Theoretical Intensities of Transitions Isoelectronic with Carbon 1

Transition $2s^2 2p^2 - 2s2p^3$	Ti XVII λ	Ti XVII A	Ti XVII I	Cr XIX λ	Cr XIX A	Cr XIX I	Fe XXI λ	Fe XXI A	Fe XXI I	Co XXII λ	Co XXII A	Co XXII I	Ni XXIII λ	Ni XXIII A	Ni XXIII I
$^3P_1 - ^5S_2$	326.4±0.2 H	5.3+6 a	9.4+0 f	280.2±0.2 H	1.38+7b	9.7+0 h	242.07±0.06 E	3.4+7 c	8.5+0 g	225.39±0.10 H	5.2+7 e	7.5+0 j	209.98±0.11 H	7.9+7 b	5.9+0 h
$^3P_2 - ^5S_2$	356.7±0.3 H	7.7+6 a	1.35+1 f	310.4±0.2 H	1.6+7 b	1.14+1 h	270.52±0.06 E	3.3+7 c	8.3+0 g	252.48±0.13 H	4.6+7 e	6.6+0 j	235.57±0.14 H	6.3+7 b	4.7+0 h
$2s^2 2p^2$															
$(^3P_1 - ^1S_o)$	470.2±0.4 G	2.5+4 d	3.1+1 f	398.0±0.3 G	6.1+4 d	2.5+1 h	335.9±0.2 G	1.38+5 d	1.8+1 g	308.0±0.2 G	2.0+5 d	1.24+1 j	282.3±0.2 G	2.9+5 d	6.0+0 h
$(^3P_1 - ^1D_2)$	898±2 G	1.9+3 d	2.6+1 f	729.9±1.1 G	5.8+3 d	4.4+1 h	587.5±0.7 G	1.6 +4d	6.0+1 g	523.4±0.5 G	2.6+4 d	5.7+1 j	465.0±0.5 G	4.2+4 d	4.3+1 h
$(^3P_2 - ^1D_2)$	1172±3 G	2.3+3 d	3.1+1 f	977±2 G	6.0+3 d	4.6+1 h	788.6±1.2 G	1.5+4 d	5.5+1 g	697.1±1.0 G	2.4+4 d	5.1+1 j	612.2±0.9 G	3.6+4 d	3.7+1 h
$(^3P_o - ^3P_1)$	3370.6±0.1 D (3371.6±0.1)	4.5+2 d	1.02+1 f	2097±7 G (2097±7)	1.8+3 d	4.1+1 h	1354.08±0.05 F	6.5+3 d	1.47+2 g	1104±2 G	1.19+4d	2.0+2 j	913±2 G	2.1+4 d	2.3+2 h
$(^3P_1 - ^3P_2)$	3834.6±0.3 D (3835.7±0.3)	2.2+2 d	7.1+0 f	2884±13 G (2885±13)	4.6+2 d	1.7+1 h	2303±8 G (2304±8)	8.3+2 d	2.6+1 g	2100±9 G (2100±9)	1.05+3d	3.2+1 j	1933±8 G	1.29+3d	3.8+1 h

Wavelengths given in Å.
Estimated wavelength accuracy is ±0.03Å unless otherwise stated.
Wavelengths above 2000Å are in air (Vacuum wavelengths given in brackets).
Transition probabilities given in sec^{-1}.
Theoretical intensities have units of photons $sec^{-1} sr^{-1}$ per ion number.
Theoretical intensities are calculated for an electron density of $4 \times 10^{13} cm^{-3}$ and for the temperatures of maximum ion abundance under ionisation equilibrium.

A - Laboratory observations listed by Fawcett (1975).
B - Laboratory observation of Fawcett et al (1974).
C - Laboratory observations listed by Lawson and Peacock (1980a).
D - New laboratory observations.
E - Solar flare observations of Dere (1978).
F - Solar flare observation of Sandlin et al (1977)
G - Predictions made using data from Edlén (1972) and Lawson and Peacock (1980a) and appropriate solar flare and tokamak observations.
H - Predictions made using data from Dere (1978), Lawson and Peacock (1980a, 1980b) and Ridgeley and Burton (1972).
J - Predictions made using data from sources A and G.

a - Transition probabilities listed by Bhatia et al (1980).
b - Transition probabilities listed by Feldman et al.(1980).
c - Transition probabilities of Mason et al.(1979).
d - Transition probabilities given by Nussbaumer and Rusca (1979).
e - Transition probabilities found using data from Bhatia et al(1980), Feldman et al(1980) and Mason et al(1979) in conjunction with own calculations.
f - Theoretical intensities obtained from data of Bhatia et al(1980) together with transition probabilities as referenced.
g - Theoretical intensities found from data of Feldman et al(1979) together with transition probabilities as referenced.
h - Theoretical intensities obtained from data of Feldman et al (1980) together with transition probabilities as referenced.
j - Theoretical intensities found by graphical interpolation.

TABLE 5. Wavelengths, Transition Probabilities and Theoretical Intensities of Transitions Isoelectronic with Boron I

Transition $2s^2 2p - 2s 2p^2$	Ti XVIII λ	Ti XVIII A	Ti XVIII I	Cr XX λ	Cr XX A	Cr XX I	Fe XXII λ	Fe XXII A	Fe XXII I	Co XXIII λ	Co XXIII A	Co XXIII I	Ni XXIV λ	Ni XXIV A	Ni XXIV I
$^2P_{1/2} - {}^2P_{3/2}$	133.86 A	5.4+9 a	2.2+2 f	116.06 B	6.0+9 d	1.28+2 h	100.78 B	6.5+9 c	6.1+1 g	93.89 B	6.8+9 e	4.3+1 j	87.50 B	7.0+9 d	2.8+1 h
$^2P_{1/2} - {}^2P_{1/2}$	136.27 A	5.6+9 a	1.26+2 f	117.96 B	3.9+9 d	4.4+1 h	102.23 B	2.7+9 c	1.18+1 g	95.15 B	2.4+9 e	5.9+0 j	88.54 B	2.0+9 d	2.9+0 h
$^2P_{3/2} - {}^2P_{3/2}$	144.76 A	3.3+10a	1.33+3 f	128.42 B	3.9+10d	8.3+2 h	114.41 B	4.6+10c	4.3+2 g	108.03 B	5.1+10e	3.2+2 j	102.11 B	5.5+10d	2.2+2 h
$^2P_{3/2} - {}^2P_{1/2}$	147.58 A	2.5+10a	5.7+2 f	130.76 B	3.0+10d	3.4+2 h	116.28 B	3.6+10c	1.5+2 g	109.70 B	3.9+10e	9.5+1 j	103.53 B	4.2+10d	6.0+1 h
$^2P_{1/2} - {}^2S_{1/2}$	148.42 A	2.6+10a	8.4+2 f	131.50 B	3.2+10d	8.6+2 h	117.17 B	4.0+10c	1.01+3 g	110.71 B	4.3+10e	1.04+3 j	104.64 B	4.7+10d	1.05+3 h
$^2P_{3/2} - {}^2S_{1/2}$	161.94±0.08 F	1.41+8b	4.6+0 f				136.01 B	1.18+8 b	3.0+0 g	130.93±0.04 F	2.6+8 e	6.2+0 j	126.22±0.04 F	4.4+8 e	9.6+0 h
$^2P_{1/2} - {}^2D_{3/2}$	179.87 A	6.4+9 a	8.4+2 f	156.01 B	8.4+9 d	8.2+2 h	135.78 B	1.12+10c	9.1+2 g	126.82 B	1.29+10e	9.1+2 j	118.52 B	1.5+10d	8.6+2 h
$^2P_{3/2} - {}^2D_{5/2}$	197.83 A	4.7+9 a	8.9+2 f	175.42 B	5.5+9 d	4.8+2 h	155.92 B	6.4+9 c	1.8+2 g	147.09 B	6.9+9 e	1.02+2 j	138.80 B	7.5+9 d	5.7+1 h
$^2P_{3/2} - {}^2D_{3/2}$	200.11±0.12 F	1.7+8 b	2.2+1 f	179.20 B	9.5+7 b	9.3+0 h	161.75 B	2.8+7 b	2.3+0 g						
$^2P_{1/2} - {}^4P_{3/2}$	301.9±0.3 F	3.9+5 a	3.6+0 f	255.54±0.13 F	8.8+5 d	2.9+0 h	216.91±0.09 F	1.9+6 c	2.0+0 g	200.21±0.08 F	2.6+6 e	1.8+0 j	184.90±0.10 F	3.7+6 d	1.8+0 h
$^2P_{1/2} - {}^4P_{1/2}$	324.9±0.3 F	1.8+7 a	1.41+1 f	282.1±0.2 F	3.9+7 d	2.4+1 h	246.54±0.12 F	8.1+7 c	3.3+1 g	231.64±0.11 F	1.13+8e	3.4+1 j	218.39±0.14 F	1.6+8 d	3.2+1 h
$^2P_{3/2} - {}^4P_{5/2}$	330.6±0.3 F	1.38+7 a	4.2+1 f	287.7±0.2 F	3.5+7 d	3.9+1 h	252.80±0.13 F	6.8+7 c	2.0+1 g	237.79±0.11 F	9.6+7 e	1.5+1 j	223.99±0.15 F	1.35+8 d	1.13+1 h
$^2P_{3/2} - {}^4P_{3/2}$	363.7±0.4 F	2.4+6 a	2.2+1 f	324.3±0.2 F	4.6+6 d	1.6+1 h	291.7±0.2 F	8.2+6 c	8.7+0 g	277.8±0.2 F	1.06+7 e	7.4+0 j	265.0±0.2 F	1.36+7 d	6.4+0 h

TABLE 5.(Continued) Wavelengths,Transition Probabilities and Theoretical Intensities of Transitions Isoelectronic with Boron 1

Transition	Ti XVIII			Cr XX			Fe XXII			Co XXIII			Ni XXIV		
$2s^2 2p - 2s 2p^2$	λ	A	I	λ	A	I	λ	A	I	λ	A	I	λ	A	I
$^2P_{3/2} - {}^4P_{1/2}$	397.6±0.5 F	6.2+6 a	5.0+0 f	368.2±0.3 F	1.00+7 d	6.2+0 h	348.0±0.2 F	1.41+7 c	5.7+0 g	342.2±0.2 F	1.6+7 e	4.8+0 j	339.6±0.3 F	1.7+7 d	3.6+0 h
$2s^2 2p$															
$(^2P_{1/2} - {}^2P_{3/2})$	1777.95±0.10 D	1.5+3 a	7.1+1 f	1205.8±0.6 E	4.9+3d	1.7+2h	845.55±0.1 C	1.40+4 c	2.4+2 g	717.0±0.8 E	2.3+4 e	2.5+2 j	611.9±0.8 E	3.7+4 d	2.5+2 h

Wavelengths given in Å.
Estimated wavelength accuracy is ± 0.03Å unless otherwise stated.
Transition probabilities given in sec^{-1}.
Theoretical intensities have units of photons $sec^{-1} sr^{-1}$ per ion number.
Theoretical intensities are calculated for an electron density of $4 \times 10^{13} cm^{-3}$ and for the temperatures of maximum ion abundance under ionisation equilibrium.

A - Laboratory observations listed by Fawcett (1975).
B - Laboratory observations listed by Lawson and Peacock (1980a).
C - Laboratory observation of Suckewer and Hinnov (1979).
D - New laboratory observation.
E - Predictions made using data from Edlén (1977) and Lawson and Peacock (1980a) and wavelength of observation C.
F - Predictions made using data from Fawcett (1975) and Lawson and Peacock (1980a).

a - Transition probabilities listed by Bhatia et al (1980).
b - Transition probabilities of Dankwort and Trefftz (1978).
c - Transition probabilities listed by Feldman et al (1979).
d - Transition probabilities listed by Feldman et al (1980).
e - Transition probabilities found using data from Dankwort and Trefftz(1978) or from Feldman et al(1979,1980) in conjunction with own calculations.
f - Theoretical intensities obtained from data of Bhatia et al.(1980) together with transition probabilities as referenced.
g - Theoretical intensities found from data of Feldman et al(1979) together with transition probabilities as referenced.
h - Theoretical intensities obtained from data of Feldman et al.(1980) together with transition probabilities as referenced.
j - Theoretical intensities found by graphical interpolation.

TABLE 6. Wavelengths, Transition Probabilities and Theoretical Intensities of Transitions Isoelectronic with Beryllium I

Transition	Ti XIX λ	Ti XIX A	Ti XIX I	Cr XXI λ	Cr XXI A	Cr XXI I	Fe XXIII λ	Fe XXIII A	Fe XXIII I	Co XXIV λ	Co XXIV A	Co XXIV I	Ni XXV λ	Ni XXV A	Ni XXV I
$2s^2-2s2p$															
$^1S_o-^1P_1$	169.59 A	1.43+10 a	4.4+3 d	149.90 A	1.7+10 b	3.5+3 e	132.87 A	2.0+10 b	2.9+3 e	125.17 A	2.2+10 c	2.6+3 f	117.95 A	2.4+10 b	2.4+3 e
$^1S_o-^3P_1$	328.34±0.05 A	1.35+7 a	1.25+2 d	293.17±0.04 A	2.7+7 b	1.13+2 e	263.74±0.03 A	4.9+7 b	1.22+2 e	250.78±0.03 A	6.4+7 c	1.24+2 f	238.81±0.03 A	8.4+7 b	1.22+2 e
$2s2p-2p^2$															
$^3P_2-^1D_2$	175.32 A	1.40+9 a	6.0+0 d	154.61 A	2.7+9 b	6.2+0 e	136.50 A	4.7+9 b	4.9+0 e	128.25 A	5.9+9 c	3.8+0 f	120.50 A	7.4+9 b	2.6+0 e
$^3P_1-^3P_2$	189.47 A	3.4+9 a	2.8+1 d	165.03 A	4.3+9 b	1.6+1 e	144.39 A	5.4+9 b	5.0+0 e	135.23 A	6.1+9 c	3.8+0 f	126.73 A	7.0+9 b	3.2+0 e
$^3P_o-^3P_1$	193.53 A	4.2+9 a	2.6+1 d	168.62 A	5.2+9 b	1.6+1 e	147.27 A	6.6+9 b	1.00+1 e	137.71 A	7.4+9 c	7.3+0 f	128.80 A	8.3+9 b	5.0+0 e
$^3P_1-^3P_1$	199.89 A	2.8+9 a	1.8+1 d	175.43 A	3.4+9 b	1.04+1 e	154.33 A	4.2+9 b	6.4+0 e	144.83 A	4.6+9 c	4.6+0 f	135.96 A	5.1+9 b	3.1+0 e
$^3P_2-^3P_2$	206.12 A	7.1+9 a	5.7+1 d	184.47 A	7.6+9 b	2.8+1 e	166.71 A	7.9+9 b	7.2+0 e	158.99 A	8.0+9 c	5.0+0 f	151.91 A	8.0+9 b	3.7+0 e
$^3P_2-^3P_1$	218.51 A	3.7+9 a	2.3+1 d	197.57 A	4.1+9 b	1.24+1 e	180.09 A	4.5+9 b	6.9+0 e	172.41 A	4.7+9 c	4.7+0 f	165.36 A	4.9+9 b	3.0+0 e
$^1P_1-^1S_o$	194.36 A	2.2+10 a	4.9+0 d	170.16 A	2.7+10 b	4.0+0 e	149.22 A	3.2+10 b	2.5+0 e	139.79 A	3.6+10 c	2.0+0 f	130.99 A	3.9+10 b	1.7+0 e
$^1P_1-^1D_2$	304.93±0.05 A	2.9+9 a	1.23+1 d	259.97±0.03 A	3.6+9 b	8.4+0 e	221.31±0.03 A	4.6+9 b	4.8+0 e	204.07 A	5.2+9 c	3.4+0 f	188.14 A	5.9+9 b	2.1+0 e

TABLE 6.(Continued)Wavelengths,Transition Probabilities and Theoretical Intensities of Transitions Isoelectronic with Beryllium I

Transition	Ti XIX			Cr XXI			Fe XXIII			Co XXIV			Ni XXV		
	λ	A	I	λ	A	I	λ	A	I	λ	A	I	λ	A	I
2s2p															
$(^3P_1-^3P_2)$	2344.6±0.2 B (2345.3±0.2)	1.00+3 a	4.1+0 d	1565.6±1.2 C	3.3+3 b	9.5+0 e	1078.9±0.6 C	9.8+3 b	1.8+1 e	905.2±0.4 C	1.6+4 c	2.1+1 f	764.6±0.3 C	2.7+4 b	1.7+1 e

Wavelengths given in Å.
Estimated wavelength accuracy is ± 0.02Å unless otherwise stated.
Wavelengths above 2000Å are in air (Vacuum wavelength given in brackets).
Transition probabilities given in sec^{-1}.
Theoretical intensities have units of photons $sec^{-1} sr^{-1}$ per ion number.
Theoretical intensities are calculated for an electron density of $4 \times 10^{13} cm^{-3}$ and for the temperatures of maximum ion abundance under ionisation equilibrium.

A - Calculated values of Edlén (1980).
B - New laboratory observation.
C - Predictions of Edlén (1980).

a - Transition probabilities listed by Bhatia et al(1980).
b - Transition probabilities listed by Feldman et al(1980).
c - Transition probabilities found using data from Feldman et al(1980)in conjunction with own calculations.
d - Theoretical intensities obtained from data of Bhatia et al(1980).
e - Theoretical intensities obtained from data of Feldman et al(1980).
f - Theoretical intensities found by graphical interpolation.

TABLE 7. Wavelengths, Transition Probabilities and Theoretical Intensities of Transitions Isoelectronic with Lithium I

Transition	Ti XX			Cr XXII			Fe XXIV			Co XXV			Ni XXVI		
2s-2p	λ	A	I	λ	A	I	λ	A	I	λ	A	I	λ	A	I
$^2S_{\frac{1}{2}}-^2P_{3/2}$	259.30 A	2.6+9 a	2.3+3 c	223.02 A	3.3+9 b	d	192.02 A	4.4+9 b	d	178.20 A	5.0+9 b	d	165.38 A	5.8+9 b	d
$^2S_{\frac{1}{2}}-^2P_{\frac{1}{2}}$	309.09 B	1.5+9 a	1.43+3 c	279.71 B	1.7+9 b	d	255.10 B	1.9+9 b	d	244.23 B	2.0+9 b	d	234.20 B	2.1+9 b	d

Wavelengths given in Å.
Estimated wavelength accuracy is ± 0.02 Å unless otherwise stated.
Transition probabilities given in sec^{-1}.
Theoretical intensities have units of photons $sec^{-1}sr^{-1}$ per ion number.
Theoretical intensities are calculated for an electron density of $4 \times 10^{13} cm^{-3}$ and for the temperature of maximum ion abundance under ionisation equilibrium.

A - Calculated values of Edlén (1979a).
B - Calculated values of Edlén (1979b).

a - Transition probabilities listed by Bhatia et al (1980).
b - Transition probabilities found using data from Bhatia et al(1980) in conjunction with own calculations.
c - Theoretical intensities obtained from data of Bhatia et al(1980).
d - Theoretical intensities not available.

TABLE 8. Identifications of Titanium Magnetic Dipole Transitions

Wavelength	Ionisation Stage	Transition
1777.95±0.10	Ti XVIII	$2s^2 2p(^2P_{\frac{1}{2}}-^2P_{3/2})$
2117.07± 0.08	Ti XIV	$2s^2 2p^5(^2P_{3/2}-^2P_{\frac{1}{2}})$
2344.6±0.2	Ti XIX	$2s2p(^3P_1-^3P_2)$
2545.08±0.08	Ti XV	$2s^2 2p^4(^3P_2-^3P_1)$
3370.6±0.1	Ti XVII	$2s^2 2p^2(^3P_0-^3P_1)$
3834.6±0.3	Ti XVII	$2s^2 2p^2(^3P_1-^3P_2)$

Wavelengths given in Å.
Wavelengths above 2000Å in air.

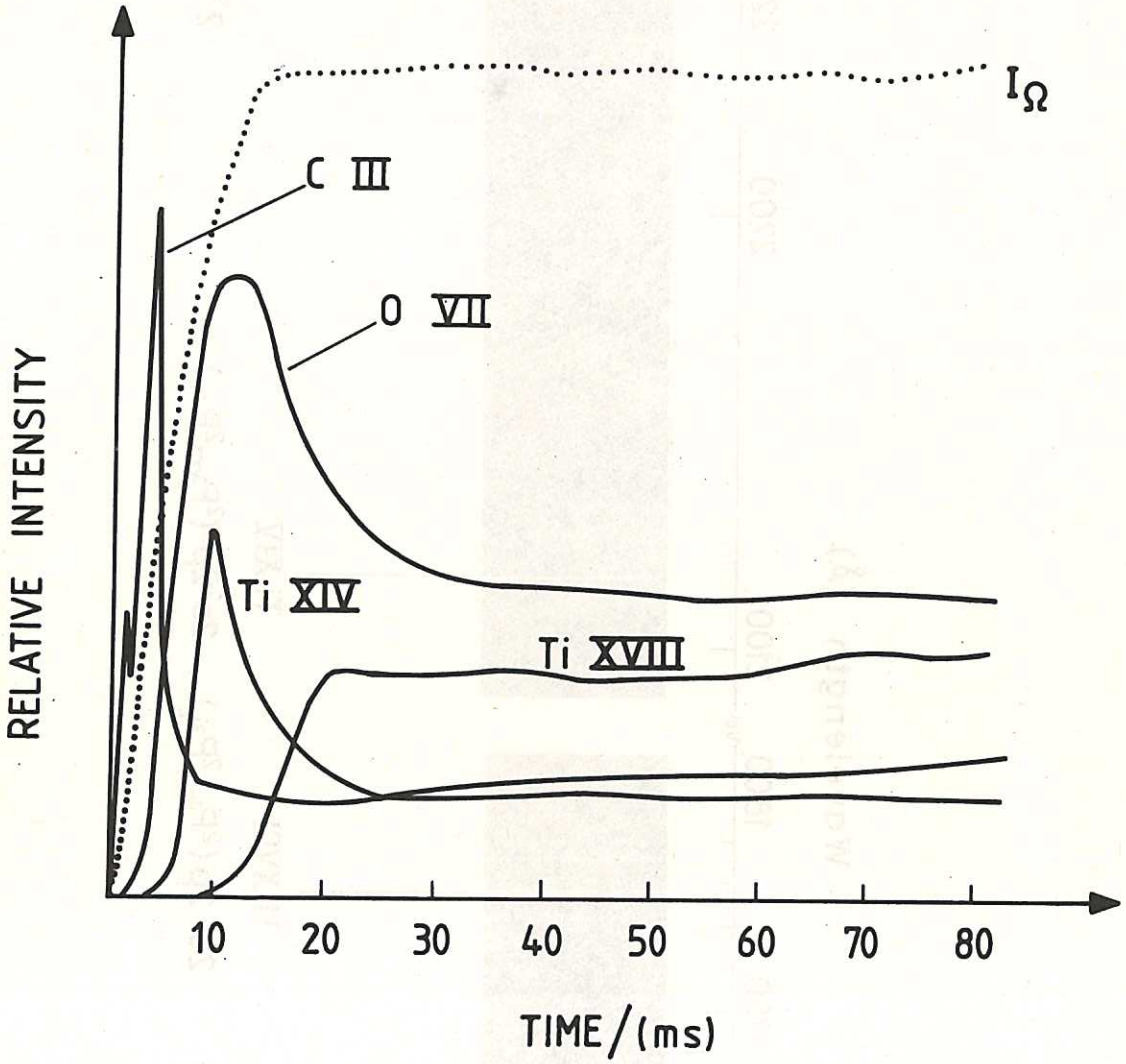

Fig.1 Temporal variation of the intensities of some DITE impurity lines, together with the ohmic heating current.

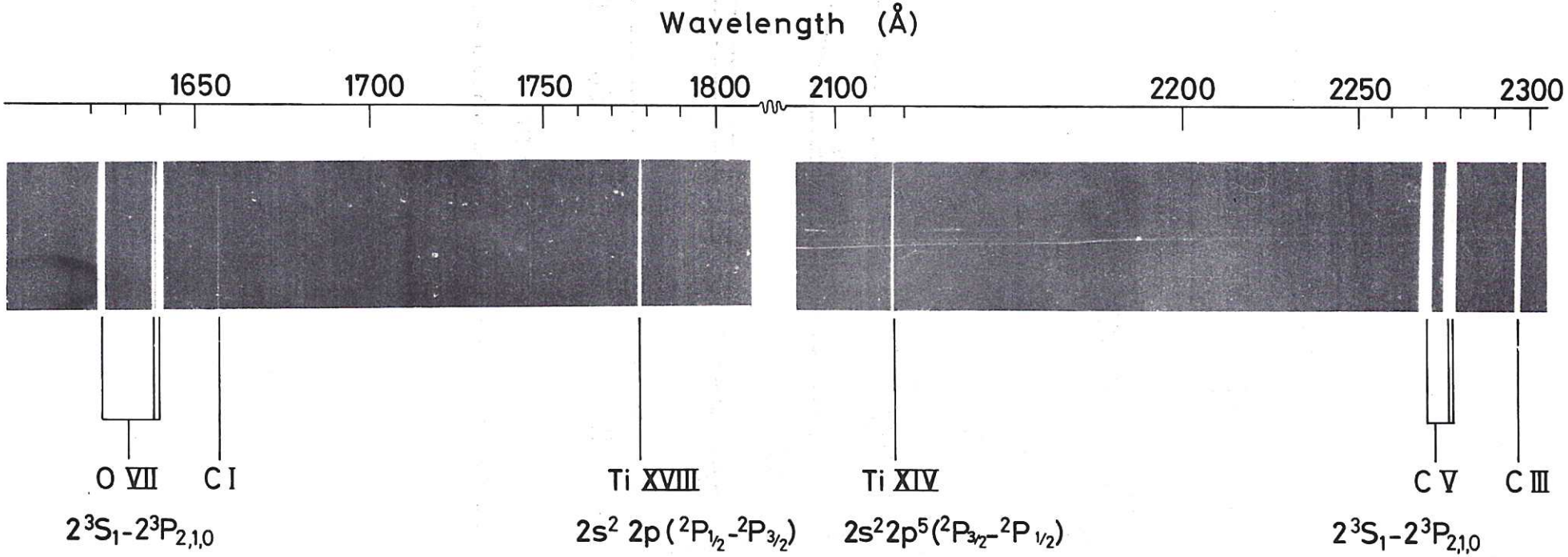

Fig.2 Near – UV spectrum from the DITE tokamak.

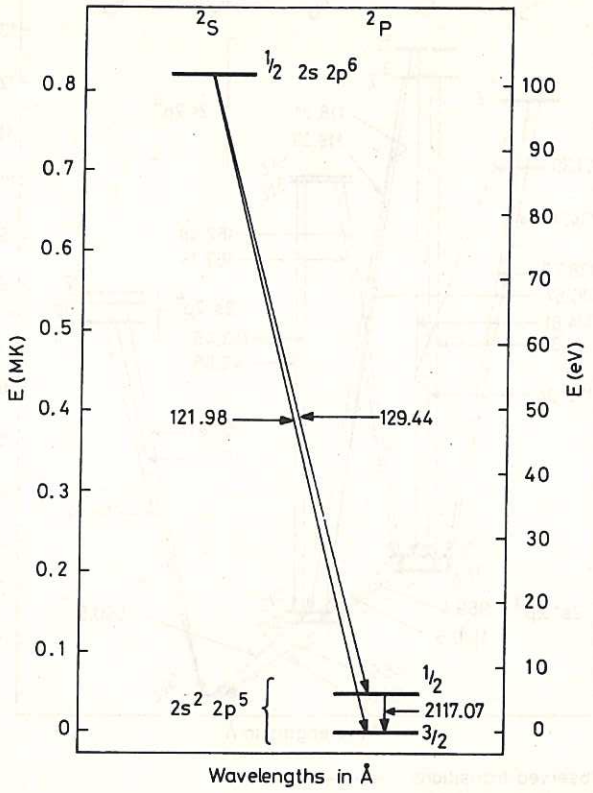

Fig.3(a) Term scheme of Ti XIV.

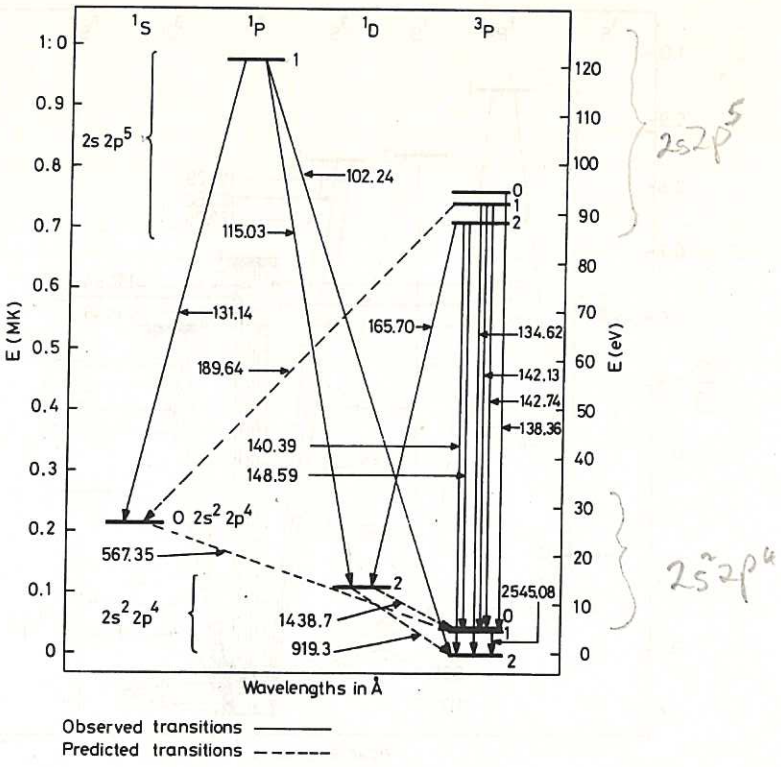

Fig.3(b) Term scheme of Ti XV.

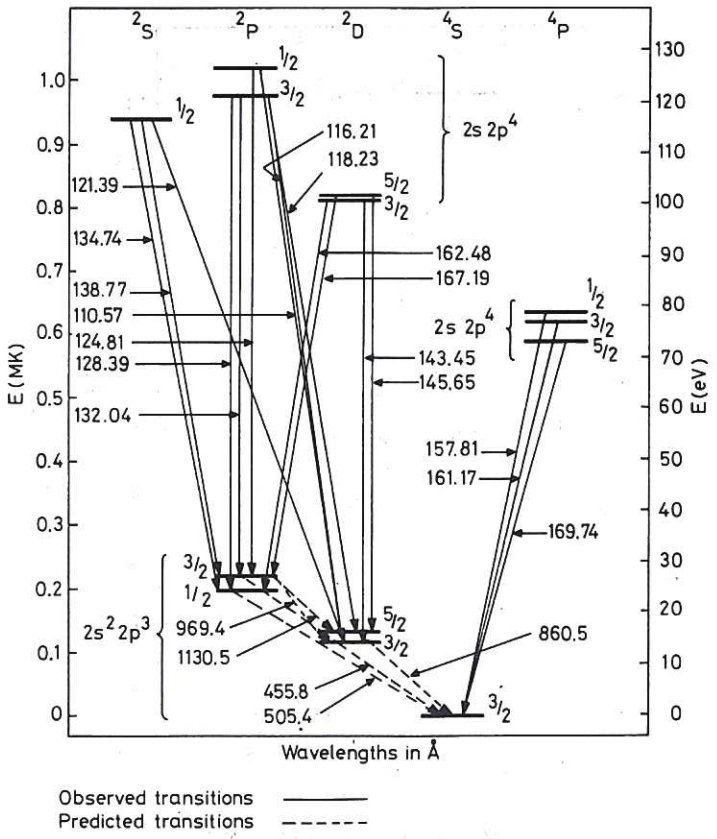

Fig.3(c) Term scheme of Ti XVI.

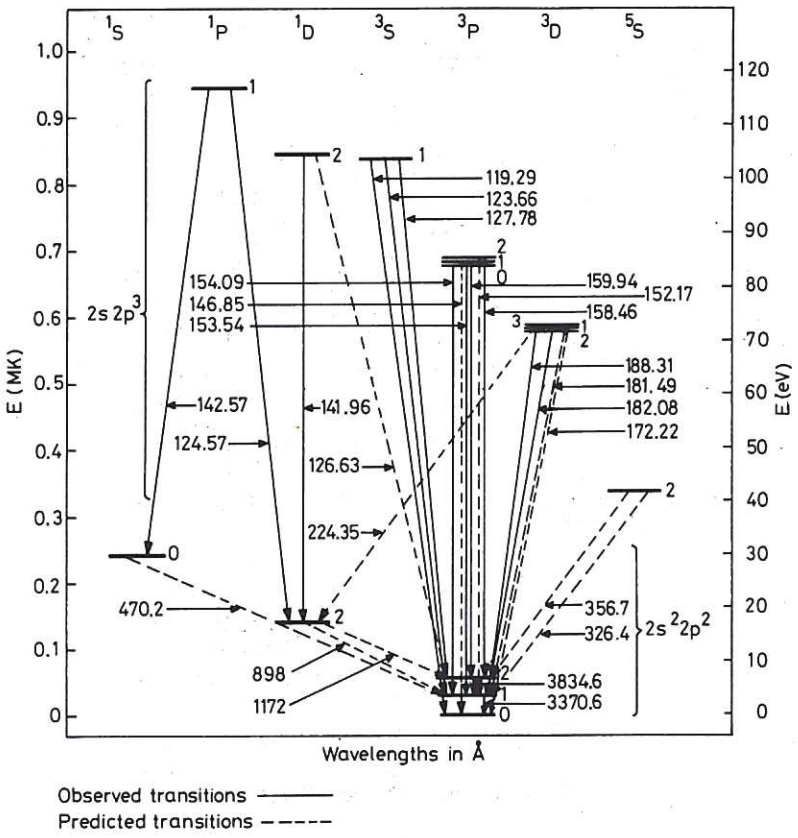

Fig.3(d) Term scheme of Ti XVII.

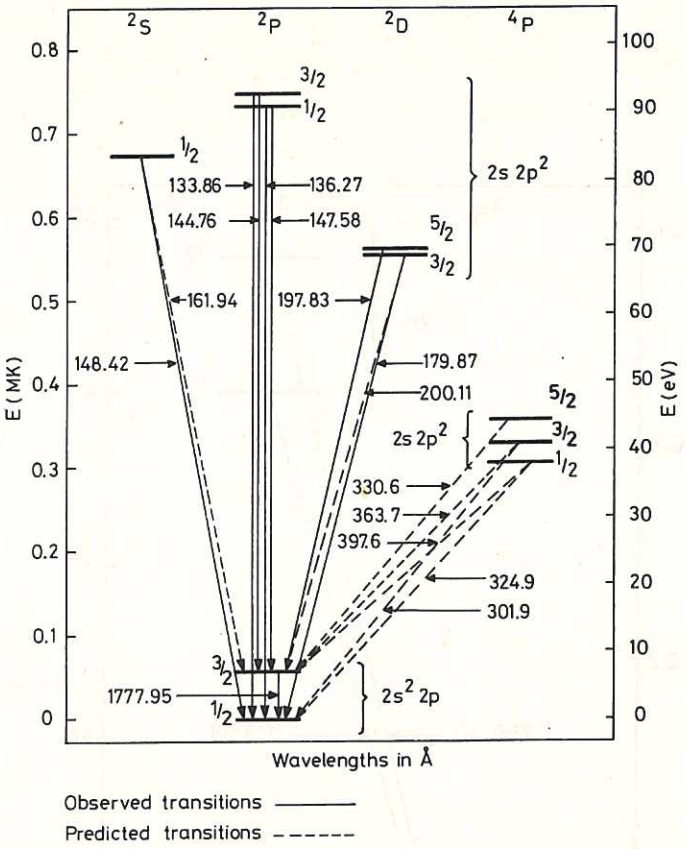

Fig.3e Term scheme of Ti XVIII.

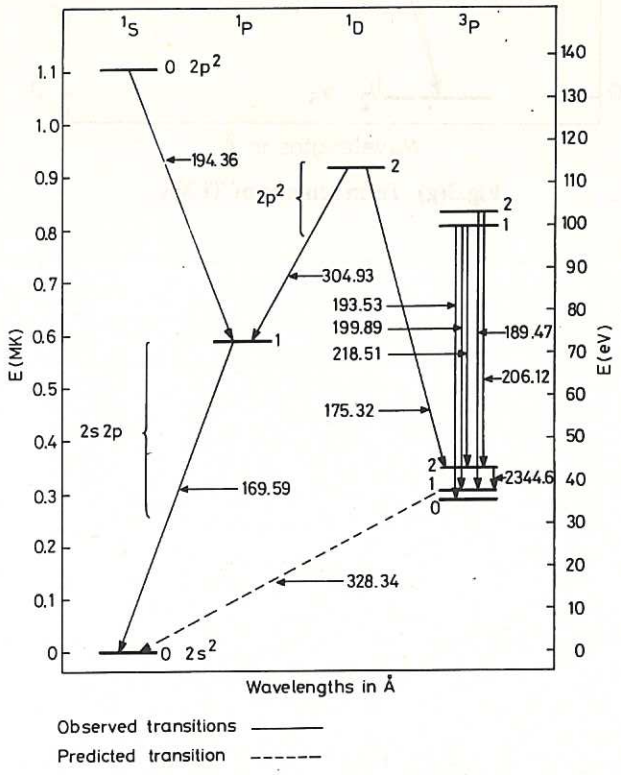

Fig.3(f) Term scheme of Ti XIX.

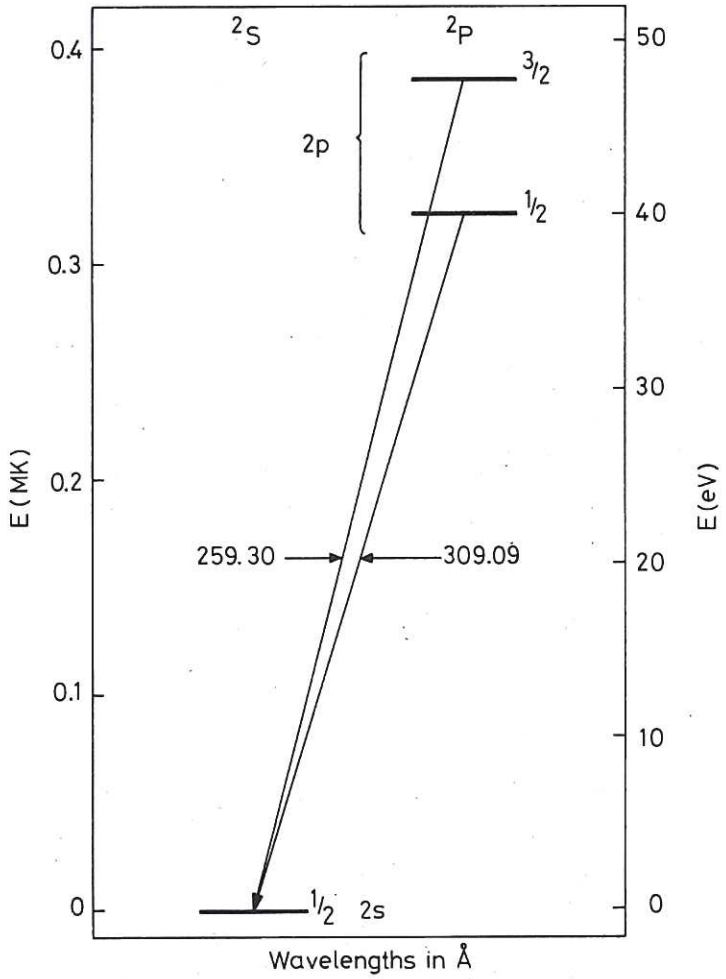

Fig.3(g) Term scheme of Ti XX.